AFRL-IF-RS-TR-1999-222
Final Technical Report
October 1999

SPREAD SPECTRUM INTERFERENCE MITIGATION WITH VARIABLE PROCESSING GAIN

Rensselaer Polytechnic Institute

Gary J. Saulnier and Zhong Ye

AIR FORCE RESEARCH LABORATORY
INFORMATION DIRECTORATE
ROME RESEARCH SITE
ROME, NEW YORK

This report has been reviewed by the Air Force Research Laboratory, Information Directorate, Public Affairs Office (IFOIPA) and is releasable to the National Technical Information Service (NTIS). At NTIS it will be releasable to the general public, including foreign nations.

AFRL-IF-RS-TR-1999-222 has been reviewed and is approved for publication.

APPROVED: Michael J. Medley

Michael J. Medley
Project Engineer
Information Connectivity

FOR THE DIRECTOR:

Warren H. Debany
Technical Advisor
Information Grid Division

If your address has changed or if you wish to be removed from the Air Force Research Laboratory Rome Research Site mailing list, or if the addressee is no longer employed by your organization, please notify AFRL/IFGC, 525 Brooks Road, Rome, NY 13441-4505. This will assist us in maintaining a current mailing list.

Do not return copies of this report unless contractual obligations or notices on a specific document require that it be returned.

REPORT DOCUMENTATION PAGE			*Form Approved* *OMB No. 0704-0188*

1. AGENCY USE ONLY *(Leave blank)*

2. REPORT DATE
OCTOBER 1999

3. REPORT TYPE AND DATES COVERED
Feb 98 - Nov 98

4. TITLE AND SUBTITLE
SPREAD SPECTRUM INTERFERENCE MITIGATION WITH VARIABLE PROCESSING GAIN

5. FUNDING NUMBERS
C - F30602-98-1-0054
PE - 61102F
PR - 2304
TA - C8
WU - 03

6. AUTHOR(S)
Gary J. Saulnier and Zhong Ye

7. PERFORMING ORGANIZATION NAME(S) AND ADDRESS(ES)
Rensselaer Polytechnic Institute
110 Eighth Street
Troy, New York 12180-3590

8. PERFORMING ORGANIZATION REPORT NUMBER
N/A

9. SPONSORING/MONITORING AGENCY NAME(S) AND ADDRESS(ES)
Air Force Research Laboratory/IFGC
525 Brooks Road
Rome NY 13441-4505

10. SPONSORING/MONITORING AGENCY REPORT NUMBER
AFRL-IF-RS-TR-1999-222

11. SUPPLEMENTARY NOTES
Air Force Research Laboratory Project Engineer: Michael J. Medley/IFGC/(315) 330-4830

12a. DISTRIBUTION AVAILABILITY STATEMENT
APPROVED FOR PUBLIC RELEASE; DISTRIBUTION UNLIMITED

12b. DISTRIBUTION CODE

13. ABSTRACT *(Maximum 200 words)*
Designing a spread spectrum signal for the worst-case channel conditions can be wasteful of system resources such as bandwidth and network throughput capacity. This report focuses on the performance of spread spectrum system based on multi-carrier modulation, also known as Orthogonal Frequency Division Multiplexing (OFDM), which provides variable processing gain by adjusting the redundancy in the signal in response to the channel conditions. A signal structure based on OFDM is defined and a technique for adapting the signal properties, including the data rate, in response to channel conditions and/or transmission requirements, is developed. Analytical and simulation results demonstrate that the signaling format can maintain a desired error rate performance over a wide range of channel conditions. The report also considers the impact of this variable signaling scheme on the upper layers of the network and, in particular, the data link layer. Classic throughput analysis for fixed and random access schemes is extended for this proposed adaptive packet radio network. The focus in on pure- ALOHA and non-persistent CSMA (NP-CSMA) systems. A large improvement in throughput is demonstrated for the adaptive system, as compared to a conventional fixed rate system, for various mobile user population profiles and radio propagation path loss models.

14. SUBJECT TERMS
Multipath, OFDM, Multi-Carrier, Spread Spectrum, Variable Processing Gain, Wireless Network

15. NUMBER OF PAGES
118

16. PRICE CODE

17. SECURITY CLASSIFICATION OF REPORT	18. SECURITY CLASSIFICATION OF THIS PAGE	19. SECURITY CLASSIFICATION OF ABSTRACT	20. LIMITATION OF ABSTRACT
UNCLASSIFIED	UNCLASSIFIED	UNCLASSIFIED	UL

Standard Form 298 (Rev. 2-89) (EG)
Prescribed by ANSI Std. 239.18
Designed using Perform Pro, WHS/DIOR, Oct 94

Contents

List of Tables

List of Figures

Chapter 1

Introduction

1.1 Overview

The primary objective of this effort was to develop techniques for using multi-carrier modulation, also known as Orthogonal Frequency Division Multiplexing (OFDM), to provide variable data rate communications through a channel characterized by multipath and interference. The investigation included both analysis and simulation-based performance evaluation. The new techniques were implemented using the Signal Processing WorkSystem (SPW) from the Alta Group of Cadence Design Systems. Both analytical results and Monte Carlo simulation were used to characterize system behavior and to obtain and verify performance results.

The investigation focused on two major areas. Initial work focused on the physical layer of the network. A signal structure based on OFDM was defined and a technique for adapting the signal properties, including the data rate, in response to channel conditions and/or transmission requirements, was developed. In particular, in a favorable channel, the system would operate much like the conventional OFDM system where different data bits are transmitted on different carriers yielding high throughput. In a severe interference

channel, the system would operate like the spread spectrum OFDM system, in which the spectral spreading is accomplished by putting the same data on all the carriers, sacrificing throughput to provide the needed processing gain to overcome the jamming. In most cases, the system would operate between these two extremes, providing sufficient processing gain to mitigate the channel effects while maximizing throughput. The behavior of the control strategy across large variation of channel conditions was studied.

The second area of the investigation studied the impact of this variable signaling scheme on the upper layers of the network, in particular, the focus was on throughput optimization from the data link layer point of view. Classic throughput analysis for fixed and random access schemes was extended for this proposed adaptive packet radio network. The focus was on pure-ALOHA and nonpersistent CSMA (NP-CSMA) systems. A large improvement in throughput is demonstrated for the adaptive system, as compared to the conventional fixed rate system, for various mobile user population profiles and radio propagation path loss models.

As a result of this effort, the adaptive signaling scheme based on OFDM was not only able to deliver excellent BER performance, a critical benchmark in any physical layer criterion, but much more importantly, it was able to boost the throughput from the network point of view and increase the total resource utilization tremendously.

1.2 Publications

A number of publications have resulted from this effort:

- Saulnier, G. J., Ye, Z. and Medley, M. J., "Performance of a Spread Spectrum OFDM System in a Dispersive Fading Channel with Interference", Conference Record of the IEEE Military Communications Conference, October, 1998.

- Saulnier, G. J., Ye, Z. and Medley, M. J., "Joint Interference Suppression and Multipath Mitigation in Direct Sequence and OFDM Spread Spectrum Systems", Conference Record of Seventh Communication Theory Mini-Conference, November, 1998.

- Ye, Z., Saulnier, G. J., Lee, D. and Medley, M. J., "Anti-jam, Anti-Multipath Adaptive OFDM Spread Spectrum System", Conference Record of Thirty Second Annual Asilomar Conference on Signals, Systems and Computers, November, 1998.

- Saulnier, G. J., Ye, Z., Vastola, K. S. and Medley, M. J., "Throughput Analysis for a Packet Radio Network Using Variable Rate OFDM Signaling", Conference Record of the IEEE International Conference on Communications, June, 1999.

- Saulnier, G. J., Ye, Z., Lee, D. and Medley, M. J., "A Rate-Adaptive Coded OFDM (RA-OFDM) Spread Spectrum System for Tactical Radio Networks", Conference Record of Eighth Communication Theory Mini-Conference, June, 1999.

1.3 Report Organization

The remainder of the report consists of four chapters. Chapter 2 presents a survey of communication systems for packet radio networks. Characteristics of the Tactical Wireless Communications Channels are outlined and the corresponding channel models for this effort are defined. Since the whole effort was oriented toward using an OFDM-based scheme for a packet radio network, the remainder of the chapter is dedicated to thoroughly introducing OFDM and its variants as well as packet radio network issues.

The rate adaptive OFDM modulation scheme is introduced in Chapter 3. It is compared to other conventional rate adaptation approaches and

presented as a unifying modulation across a large range of channel conditions. The adaptation scheme as well as the packet structure are then introduced. System performance results for a variety of channel conditions including AWGN, static multipath, time-varying frequency selective and frequency non-selective Rayleigh fading show that a desired BER performance can be maintained through adjustment of the processing gain.

Chapter 4 extends the contribution of the adaptive signaling beyond the physical layer. Throughput analysis of the proposed adaptive packet radio network is performed. The focus is on simple access schemes such as pure-ALOHA and non-persistent CSMA. The great potential of the adaptive signaling is demonstrated and it serves as a door opener to a domain of new research opportunity.

Finally, Chapter 5 presents a summary of the work presented in this report.

Chapter 2

Survey of Communications Systems for Packet Radio Networks

Almost two decades have passed since the first generation mobile cellular telecommunication services using analog frequency modulation/frequency division multiple access (FM/FDMA) started. Today, in addition to analog systems, the second generation digital cellular systems are in widespread use. The technical motivation for the first and second generation mobile cellular networks was mainly to increase system capacity for voice services. At the turn of the century, we are experiencing the ever expanding use of the Internet with a rapid growth of people's need for multimedia communications services including voice, data and images. How to deliver high speed and reliable multimedia traffic to people anywhere and anytime has become the technical challenge as the third and fourth generation mobile telecommunication systems evolve.

The need for moving from legacy analog systems to state-of-the-art digital systems is even more urgent in the military world. Victory in the 21st

Century battlespace will be characterized by the effective leveraging of information technology to rapidly mass the effects of dispersed firepower, rather than relying exclusively on the physical massing of weapons and forces that was the primary method employed in the past. Digitization is a means to that end.

Digitization allows the warrior to communicate vital battlefield information instantly, rather than through a slow voice radio or even slower liaison efforts. It provides the warrior with a horizontally and vertically integrated digital information network that supports unity of battlefield fire and maneuvers and assures command and control decision-cycle superiority. The intent is to create a simultaneous, appropriate picture of the battlespace based on common data collected through networks of sensors, command posts, processors, and weapon platforms. This allows participants to aggregate relevant information and maintain an up-to-date awareness of what is happening around them [1].

Both the commercial and military wireless communications systems share the requirement of delivering high quality, high speed multimedia traffic and should be highly flexible to accommodate changing traffic patterns as well as channel conditions. Beside providing a significant level of immunity to time-varying multipath fading, military systems face a constant challenge of intentional interference and/or interception. Additionally, they need to account for the possibility of high priority messages which might require rapid network access and/or high bandwidth. If a network is expected to operate in a military environment, it clearly must have some of these attributes.

To provide some perspective, the following is a summary of some of the requirements for the future tactical wireless networks:

- Support mobility, the ability to communicate while in motion, and a seamless network that interconnects individual human subscribers with moving vehicles, with aircraft, and with static and commercial

networks.

- Provide secure, survivable low probability of intercept(LPI) and jam resistant (AJ) capabilities in support of system network operation.
- Provide reliable service in a highly dispersive multipath environment.
- Provide variable Quality of Service (QoS), i.e. accommodate various services with possibly different priority, data rates, error performance and delay requirements. The networks should support data traffic and possibly voice and video traffic.
- High speed, at least comparable to today's Ethernet, with a route for upgrading to higher speed into the future.
- Low complexity and low power consumption.
- Easy and fast installation and deployment. Little or no site planning required.

This report first discusses some of the distortions introduced by the channel and the approaches that are taken to mitigate their effect on performance. Later, a rate-adaptive modulation scheme is presented as a possible solution to the physical layer problem in a tactical wireless network. This technique is evaluated through the use of bit-error-rate performance. Finally, the performance of several network configurations using the rate-adaptive scheme is investigated and this performance is compared to that of a fixed-rate system.

2.1 Characteristics of Tactical Wireless Communications Channels

The radio channel is the medium for tetherless local transmission. Wireless networks typically use the microwave frequencies, which occupy the 10^9 to

10^{12} Hz portion of the frequency spectrum. The effective design, assessment, and installation of a radio network requires an accurate characterization of the channel. Having an accurate channel model for each frequency band, including key parameters and a detailed mathematical model of the channel, enables the designer or user of a wireless system to predict signal coverage, achievable data rate, and the specific performance attributes of alternative signaling and reception schemes. The channel conditions experienced by both the base stations and/or the mobiles are typically much more severe than their commercial applications counterparts due to the following reasons:

- Networks can be on the move
- Much higher vehicle speed
- Severe and unpreditable terrain profile
- Intentional jamming

In addition, the following stringent requirements of a military communications network make an optimum design even more challenging:

- Higher mobility support
- Larger LPI and AJ margin
- Guaranteed delivery of high priority command messages

Interference mitigation is therefore important for military applications. There are two distinct types of interference that will be encountered within the network, multipath interference and intentional interference. The following studies the models of these interferences.

2.1.1 Multipath

Reflection, Diffraction, and Scattering

The signals we send over the air waves get severely distorted between the transmitter and the receiver due to reflection, diffraction, and scattering. Reflections of electro-magnetic waves off objects interfere constructively and destructively with the transmitted wave and with each other. When these objects are large compared to the wavelength of the electro-magnetic wave, the multipaths taken by the waves are called reflections. Occasionally, an impenetrable object will block the direct line-of-sight path between the transmitter and the receiver, resulting in only reflected waves reaching the receiver. This effect, shadow fading, results in the received signal power being less than the mean expected through path loss computations. When the propagating wave bounces off small objects on the order of or less than the wavelength of the propagating wave, the multipath effect is called scattering. Reflection, diffraction, and scattering are collectively called multipath propagation [2].

Impulse Response

Because the transmitted radio signal propagates along multipaths, a transmitted impulse will be smeared out into a broad impulse response. We can express the radio channel impulse response at a given instance in time between a particular transmitter and receiver as the sum of the paths of all the individual rays take:

$$h(\tau, t) = \sum_{i=1}^{L} \beta_i(t) e^{j\phi_i(t)} \delta(t - \tau_i) \tag{2.1}$$

where the $\beta_i(t)$ and $\phi_i(t)$ represent the amplitude and phase of the i-th path arriving at delay τ_i. (2.1) is widely used for statistical modeling of both indoor and outdoor radio propagation.

Evidently, the time variation, called fading, is caused by the interference between multiple versions of a transmitted signal arriving at slightly different times. These waves combine noncoherently at the receiver which produce a resultant signal which can vary widely in phase and amplitude.

Channel Correlation Functions and Power Spectra

We shall now define a number of correlation functions and power spectral density functions that characterize the fading multipath channel [3].

Assuming the impulse response $h(\tau, t)$ is wide-sense-stationary, we define the autocorrelation function of $h(\tau, t)$ as

$$\phi_c(\tau_1, \tau_2; \Delta t) = \frac{1}{2} E[h^*(\tau_1; t) h(\tau_2; t + \Delta t)]. \tag{2.2}$$

Most radio transmissions experience so called uncorrelated scattering in which the scattering at two different delays is uncorrelated. $\phi_c(\tau_1, \tau_2; \Delta t)$ thus becomes $\phi_c(\tau_1; \Delta t)\delta(\tau_1 - \tau_2)$. If we let $\Delta t = 0$, the resulting autocorrelation function $\phi_c(\tau, 0) = \phi_c(\tau)$ is simply the average power output of the channel as a function of the time delay τ and it is called the multipath intensity profile. The range of values of τ over which $\phi_c(\tau)$ is essentially nonzero, is called the multipath delay spread and is called T_m.

A completely analogous characterization of the time-variant multipath channel can be done in the frequency domain. Given the channel impulse response $h(\tau; t)$, the frequency response $H(f; t)$ is defined as,

$$H(f; t) = \int_{-\infty}^{\infty} h(\tau; t) e^{-2\pi j \tau} d\tau. \tag{2.3}$$

The correlation in the frequency domain can be defined as

$$\begin{aligned} \phi_C(f_1, f_2; \Delta t) &= \frac{1}{2} E(H^*(f_1; t) H(f_2; t + \Delta t)) \\ &= \int_{-\infty}^{\infty} \phi_c(\tau_1; \Delta t) e^{-j2\pi \Delta f \tau_1} d\tau_1 = \phi_C(\Delta f; \Delta t). \end{aligned} \tag{2.4}$$

$\phi_C(\Delta f; \Delta t)$ is called the spaced-frequency, spaced-time correlation function of the channel. This function is the Fourier transform of the spaced-time correlation function $\phi_c(\tau; \Delta t)$.

For a slowly time-varying channel, the value of $\phi_C(\Delta f; \Delta t)$ calculated with observation times separated by Δt is the same as that found with no time separation, i.e. set $\Delta t = 0$ in (2.4). The transform relationship then becomes,

$$\phi_C(\Delta f) = \int_{-\infty}^{\infty} \phi_c(\tau) e^{-j2\pi\Delta f\tau} d\tau. \tag{2.5}$$

The relationship is depicted in Figure 2.1. Since $\phi_C(\Delta f)$ is an autocorrela-

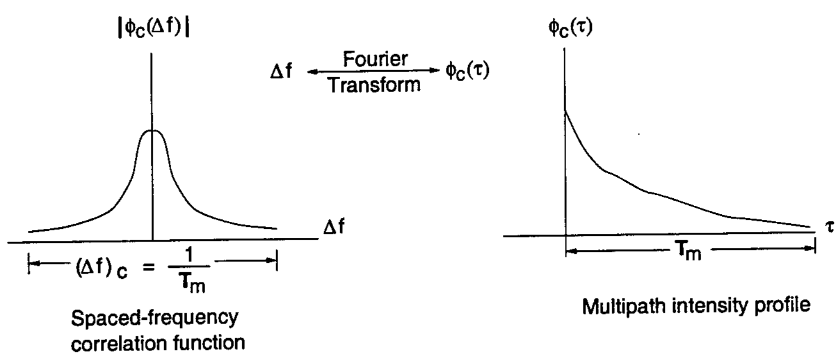

Figure 2.1: Relationship between $\phi_C(\Delta f)$ and $\phi_c(\tau)$

tion function in the frequency domain, it provides us with a measure of the frequency coherence of the channel. Since $\phi_C(\Delta f)$ and $\phi_c(\tau)$ are a Fourier transform pair, the reciprocal of the multipath spread is a measure of the *coherence bandwidth* of the channel. The coherence bandwidth is defined as the frequency separation at which the autocorrelation of the channel frequency response is essentially zero. The coherence bandwidth is related to the delay

spread as follows:

$$(\Delta f)_c \approx \frac{1}{T_m}, \tag{2.6}$$

where $(\Delta f)_c$ is the coherence bandwidth and T_m is the delay spread.

Time variation of the channel is reflected by the parameter Δt in $\phi_C(\Delta f; \Delta t)$. This time variation is evidenced as a Doppler broadening and can be quantized by defining the scattering function $S_C(\Delta f; \lambda)$, as

$$S_C(\Delta f; \lambda) = \int_{-\infty}^{\infty} \phi_C(\Delta f; \Delta t) e^{-j2\pi\lambda\Delta t} d\Delta t. \tag{2.7}$$

With Δf set to zero, $S_C(0; \lambda)$ becomes $S_C(\lambda)$, a power spectrum that gives the signal intensity as a function of the Doppler frequency λ. The range of values of λ over which $S_C(\lambda)$ is essentially nonzero is called the Doppler spread f_d of the channel. Since $S_C(\lambda)$ is related to $\phi_C(\Delta t)$ by the Fourier transform, the reciprocal of f_d is a measure of the coherence time of the channel. That is,

$$(\Delta t)_c \approx \frac{1}{f_d}, \tag{2.8}$$

where $(\Delta t)_c$ is the coherence time of the channel. The relationship is depicted in Figure 2.2.

Frequency non-selective Fading

There are several statistical models for fading channels, which describe channel variations using certain probability density functions (pdf). Rayleigh, Rician, and Nakagami-m fading are some examples. The Rayleigh fading assumes a large number of scatterers in the channel that contribute to the signal at the receiver, but no dominant line-of-sight (LOS) propagation path. On the other hand, Rician fading assumes a dominant LOS path. The Nakagami-m fading is a generalized fading characterized by the parameter m. $m = 1$ corresponds to Rayleigh fading. $m < 1$ corresponds to a fading worse than

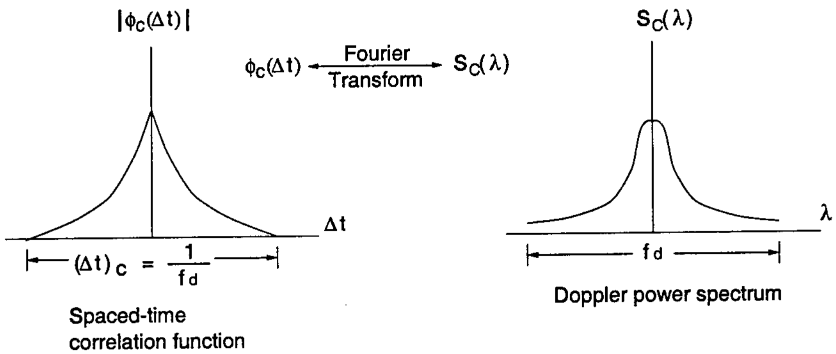

Figure 2.2: Relationship between $\phi_C(\Delta t)$ and $S_C(\lambda)$

the Rayleigh case. $m > 1$ corresponds to Rician fading and $m = \infty$ corresponds to additive white Gaussian noise channel [3].

Under most cases of the outdoor mobile communications system, the propagation path characteristics are considered to be under non line-of-sight (NLOS) conditions because a terminal is shadowed by the natural terrain and man-made constructions. Moreover, an NLOS condition is considered to be more severe than an LOS condition. Therefore, we will use Rayleigh fading as the non-selective fading channel model for this report. In Rayleigh flat fading, the channel can be modeled as a single complex multiplying factor $\alpha e^{j\theta}$, where the phase θ is uniformly distributed over $[0, 2\pi)$ and α is Rayleigh distributed. The Rayleigh probability density function is given by

$$p(r) = \frac{r}{\sigma^2} exp\left(-\frac{r^2}{2\sigma^2}\right) \quad ; r \geq 0 \tag{2.9}$$

Because the channel impulse response is just an impulse in time, the frequency response is a constant, i.e. *non-selective* or *flat* in frequency. This

is a good model when the bandwidth of the transmitted signal is much smaller than the coherence bandwidth of the channel and it is thus accurate to assume the frequency response of the channel to be constant at a given instant. The rate at which α and θ change is determined by the Doppler frequency, or equivalently, the coherence time.

There are several ways to model a Rayleigh flat fading channel. Most use a frequency spectrum based on Jakes model,

$$H(f) = \begin{cases} \frac{A}{\sqrt{1-\left(\frac{f}{f_d}\right)^2}} & |f| \leq f_d \\ 0 & |f| \geq f_d \end{cases}$$

A plot of the Jakes filter frequency response is shown in Figure 2.3.

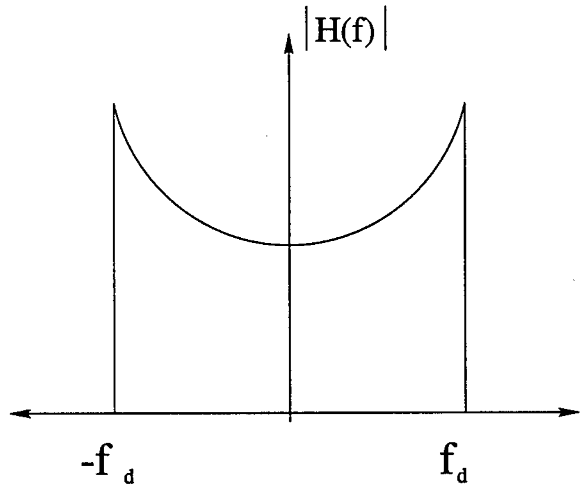

Figure 2.3: Doppler power spectrum based on Jakes model

Frequency Selective Fading

Flat fading characterizes the channel when the arrival time difference between paths is negligibly small, i.e. the coherence bandwidth is large. How-

ever, when the bandwidth of the transmitted signal is very wide, we cannot neglect the arrival time difference, especially when the time difference becomes comparable to a symbol duration. When the delay spread is long enough that delayed versions of one symbol interferes with the next symbol when it is sampled, frequency selective fading occurs. The channel frequency response will no longer be flat as in the flat fading. The longer the delay spread, the more the frequency response will vary in a given frequency band. Such a time-varying frequency-selective fading channel model is depicted in Figure 2.4. The channel consists of multiple rays spaced at sample intervals, T_c, and having a intensity profile determined by $a_1, ...a_N$. Each ray is independently Rayleigh faded with an adjustable Doppler rate.

2.1.2 Multipath Mitigation Techniques

Many schemes have been developed to help mitigate the effects of multipath, and some of them are discussed below.

- **Spatial diversity** is implemented by using multiple receive and/or transmit antennas. These antennas should be spaced far enough apart to achieve independence between branches. Ideally, the antennas only have to be $\frac{\lambda}{2}$ apart – but in practice, they are usually separated by 10λ. The military has always been interested in single-channel (i.e. antenna) techniques because they have been generally cheaper, less complex, smaller in size, and more suitable to rugged military applications than multichannel techniques [4]. Along the same line, the commercial wireless community will likely favor techniques that are inexpensive and simple to implement. For the purpose of this report, we will exclusively concentrate on single antenna receiver structure.

- **Frequency diversity** involves independently sending the same information over several frequencies simultaneously. If the frequencies are

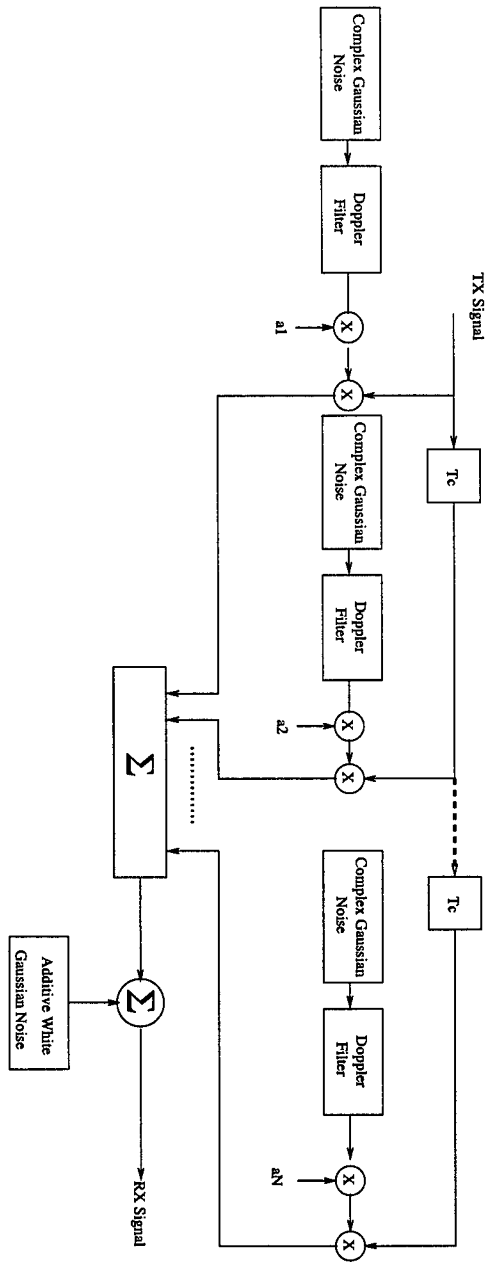

Figure 2.4: Frequency selective fading channel

separated by more than the coherence bandwidth, the channels will be independent from each other, making it very unlikely that they will all be in a fade at the same moment. For example, the coherence bandwidth is on the order of 500kHz in the mobile radio case, thus requiring that the frequencies be separated by 1-2MHz, which makes that frequency diversity much more difficult to obtain using traditional single carrier systems. Frequency diversity is thus ideally suited for multicarrier approach such as OFDM as will be discussed very shortly. By placing identical data bits on independent subcarriers, frequency diversity is achieved. In addition, frequency diversity is flexible enough to mesh with other means of diversity within the OFDM system, making it the focus of choice for this report.

- **Time diversity** involves sending the same information more than once. The trick is to wait long enough for the channel to have changed before sending the packet again. From the preceding discussion, the time spacing between diversity bits should be at least the coherence time to satisfy this condition. For this reason, time diversity is better suited for rapidly changing channels and it is often achieved through coding. For slow fading channels, there will be a significant delay before all the diversity bits can be processed for a decision to be made. The delay can be too great for some applications in this case. This limitation motivates us to pursue other means to harness the channel. The emphasis of this report, i.e. using rate adaptation to exploit the long term fluctuation of the fading channel is especially effective to handle slow time varying fading channels. In addition, time diversity is supplemented with additional means of diversity to handle other types of fading conditions, making it a viable solution for a broad range of channel conditions.

- **Polarization diversity** depends on the independence between horizontal and vertical polarization paths between the transmitter and the receiver. Because these are the only two polarizations (vertical and horizontal), this type of diversity is limited to two branches.

- **Adaptive Equalization.** This technique has become widely used in modern microwave point-to-point links and mobile radio systems to counteract ISI and improve performance [3]. Equalizer hardware can take many forms, including a tapped delay line structure and a lattice structure, though the tapped delay line type is most common. In this case the tapped delay line structure has programmable tap weights connected to each tap and to a common summing bus. This equalizer counteracts multipath distortion in the time domain by introducing its own echoes, whose phases and amplitudes are automatically adjusted to cancel the ISI produced by the channel. The same fundamental principle of estimating the ISI and canceling it can be applied to the transform domain as well, producing frequency domain equalization. An equalizer generally employs some type of adaptive algorithm to allow it to follow the variations of the channel. As a consequence, the rapid channel variations encountered when transmitter and/or receiver are moving at a high rate make it difficult for the equalizer to perform well.

- **Spread Spectrum.** Spread spectrum modulation is naturally tolerant of multipath if its bandwidth exceeds the coherence bandwidth of the channel [5]. The spread spectrum signal, in essence, provides *frequency diversity* due to its large bandwidth. A RAKE receiver is often used to exploit the multipath. [6]. The one major drawback to the use of spread spectrum, at typical WLAN data rates, is the wide bandwidth occupied by such a signal. This might become a concern for future

higher data rate services.

- **Multicarrier Modulation.** This approach mitigates multipath by reducing the effective symbol rate "seen" by the channel. It splits the data into n separate streams, which are then modulated onto a multiplex of closely-spaced carriers. Hence the symbol rate on each is reduced by the factor of n, which greatly reduces the ISI.

- **Rate Adaptive Transmission.** Yet another approach to increase data rate in the presence of multipath fading is to use a rate adaptive (RA) modem. A RA modem provides one or more "fallback" modes of operation for increased reliability of communication under degraded channel conditions. For example, in an area where we have locations of good signal quality and others of poor quality, we can operate at higher data rates in the good location and lower rates at the poor locations. The idea of rate adaptation can be implemented in various ways. One way to adjust the data rate with a fixed bandwidth is to use the multiamplitude and multiphase modulation. In this method, the number of points in the constellation is increased as the channel condition improves. The technique is often used in wireline modems. A second way to implement adaptive data rate is through variable FEC coding. In this case, the degree of redundancy introduced by the FEC coding scheme, i.e. the coding rate, is varied according to the channel conditions. In order to allow reasonable complexity at the receiver to decode the variable rate code, a rate compatible puncture code (RCPC) is often used. The third way to implement variable data rate is to combine the adaptive modulation with the variable coding scheme. An obvious disadvantage of the variable coding scheme is the narrow dynamic range of the data rate as constrained by the decoder complexity. Due to a large power fluctuations in a wireless channel,

it is difficult to reliably demodulate signal sets with large numbers of points without using complex equalization approaches. In addition to this, the military applications generally require LPI/LPD. All of these motivate us to implement the rate adaptation in a different way. We incorporate it with the spread spectrum system where the processing gain can be adjusted with the environment. Details of the concept will be introduced in the next section.

2.1.3 Intentional Interference

In this case, an attempt is being made to jam the communications link. The jamming can take many forms, including continuous tone and partial-band interference, pulsed tone and partial-band interference, pulsed broadband interference, and frequency chirps. Many interference suppression techniques have been proposed [7, 8] to improve performance in the presence of different types of jammers, particularly for direct sequence spread spectrum systems. For strong interference, it is essential that a selected modulation format be able to provide interference immunity in excess of its processing gain, meaning that some type of auxiliary interference suppression technique must be compatible with the modulation format. The interference rejection techniques also need to be adaptive because of the dynamic or changing nature of interference and channel conditions. The design of an optimum receiver requires a priori information about the statistics of the data to be processed. When complete knowledge of the signal characteristics is not available, an adaptive technique is needed. Given the interference characteristic of the tactical packet radio networks, we have proposed an adaptive filter structure that can jointly suppress multipath interference as well as intentional tone jammer. Essentially, it is an adaptive equalizer in the frequency domain, which manages to suppress both ISI and ICI caused by the multipath and

simultaneously notch out a narrowband jammer by minimizing the mean-square value of the error signal, which is defined as the difference between some desired response and the actual filter output [9, 10, 11, 12, 13].

2.2 OFDM

The principles of OFDM were first introduced about 28 years ago [14]. However, practical interest has only increased recently due in part to advances in signal processing and microelectronics. In the past, as well as in the present, this same modulation scheme is referred as multitone, multicarrier, and orthogonal frequency division multiplexing communications.

2.2.1 Conventional OFDM

The main idea behind OFDM is to split the data stream to be transmitted into N parallel streams of reduced data rate and to transmit each of them on a separate subcarrier. These carriers are made orthogonal by appropriately choosing the frequency spacing between them. Therefore, spectral overlapping among subcarriers is allowed, since the orthogonality will ensure that the receiver can separate the OFDM subcarriers, and a better spectral efficiency can be achieved than by using simple frequency division multiplexing.

In the most general form, the lowpass equivalent OFDM signal can be written as a set of modulated carriers transmitted in parallel, as follows:

$$s(t) = \sum_{n=-\infty}^{\infty} \left[\sum_{k=0}^{N-1} C_{n,k} g_k(t - nT_s) \right] \tag{2.10}$$

with

$$g_k(t) = \begin{cases} e^{j2\pi f_k t} & 0 \leq t < T_s \\ 0 & \text{otherwise} \end{cases} \tag{2.11}$$

and

$$f_k = f_0 + \frac{k}{T_s}, \; k = 0 \ldots N-1 \tag{2.12}$$

where $C_{n,k}$ is the symbol transmitted on the k-th subcarrier in the n-th signaling interval, each of duration T_s, N is the number of OFDM subcarriers, and f_k is the k-th subcarrier frequency, with f_0 being the lowest frequency to be used. The OFDM modulator and demodulator can be efficiently implemented by the inverse Fast Fourier Transform (IFFT) and Forward FFT,respectively. Figure 2.5 shows an OFDM system using a FFT.

Recent advances in digital signal processing (DSP) and very large scale integrated circuit (VLSI) technologies have paved the way for massive implementation of OFDM. One successful implementation of OFDM is in digital audio broadcasting (DAB) [15], which was developed in Europe for terrestrial and satellite broadcasting of multiple audio programs to mobile receivers. Another implementation is in asymmetric digital subscriber line (ADSL) technology that has been selected by ANSI for transmission of digitally compressed video signals over telephone lines [16]. In addition, OFDM has been adopted as the standard for digital video broadcasting (DVB) [17].

2.2.2 Spread Spectrum OFDM

OFDM can also be used as a spread spectrum modulation (OFDM-SS) [18, 19, 20, 21] wherein spectral spreading is accomplished by putting the *same data* on all the carriers, producing a spreading factor equal to the number of carriers. At the receiver, the energy from all the carriers is coherently combined to produce the decision variable. Multiple users can be supported in the same channel through Code Division Multiple Access (CDMA) [22]. In this case each user has a unique signature sequence which determines the set of carrier phases. To receive a particular signal, the receiver needs to know the signature sequence for that user in order to align the carrier phases for the coherent combining operation. Figure 2.6 is a block diagram of an OFDM-SS transmitter/receiver pair. As shown in the figure, carrier generation is

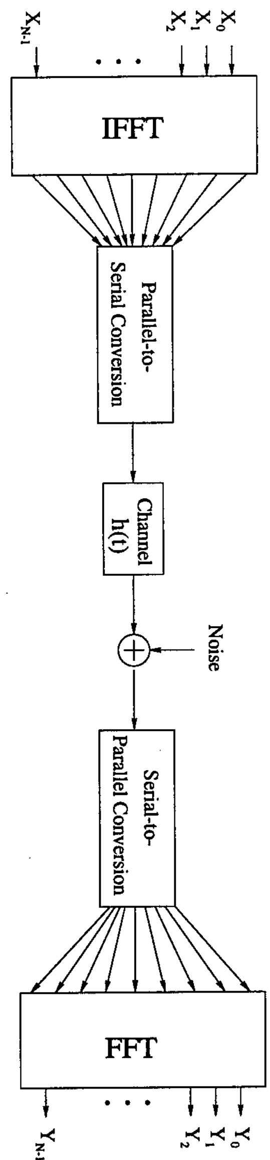

Figure 2.5: OFDM using FFT

usually performed efficiently using an inverse Fast Fourier Transform (FFT) while demodulation is performed using a forward FFT.

The use of an OFDM spread spectrum signal rather than the conventional

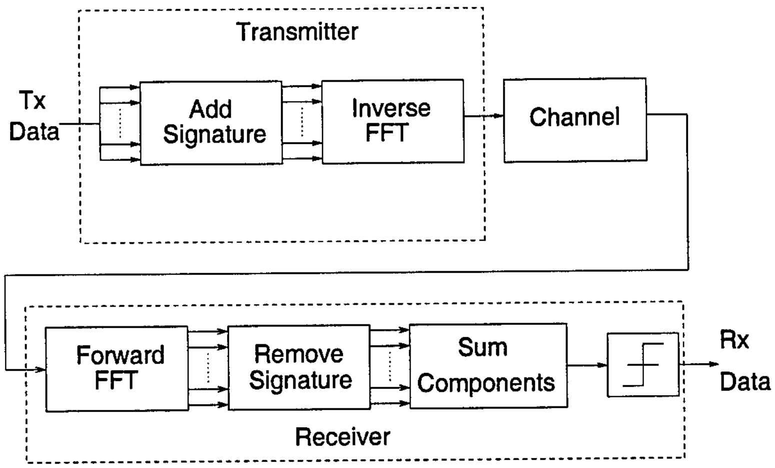

Figure 2.6: Block Diagram of an OFDM Spread Spectrum System

direct sequence signal opens up a number of possibilities:

- The transmitter can adjust the transmit spectrum in response to the jamming conditions by varying the power of each of the carriers. If some carriers are jammed, the transmitter can shift all the energy away from those carriers.

- Coding can be used in place of simply sending the same data on all the carriers. In essence a repetition code can be replaced by a much better code.

- Inserting time diversity produces a transmitted waveform that is the function of multiple data bits. Consequently, there are up to 2^M different waveforms which are chosen depending on sequence of data bits being sent. This property could make the signal more suitable for low probability of detection and low probability of intercept (LPD/LPI) applications.

The OFDM-SS system has some of the advantages of both DSSS and FHSS

systems and, what is more important, it provides an easy way to implement the rate adaptation concept we discussed earlier.

2.2.3 Equalization of OFDM signals

In addition to ISI, OFDM signals experience an additional type of interference called inter-channel interference (ICI). ICI occurs when orthogonality between subcarriers is compromised, and subcarriers within the same OFDM symbol interfere with each other. A multipath channel will produce both ISI and ICI. Traditionally, a guard interval, called cyclic prefix, is used to suppress ICI and ISI when the channel echo duration is sufficiently small. A cyclic prefix appends a copy of the last M samples of the transmitted block to the beginning of the block, as shown in Figure 2.7. This makes the linear convolution performed by the channel behave like a circular convolution [23], resulting in no spectral leakage from one sub-carrier into the neighboring bins, i.e. eliminating ICI completely. At the receiver, the cyclic prefix is removed, and the received block is processed as usual. If the cyclic prefix is made longer than the delay spread, then ISI is removed as well, since any energy from the current symbol will only interfere with the cyclic prefix of the next symbol.

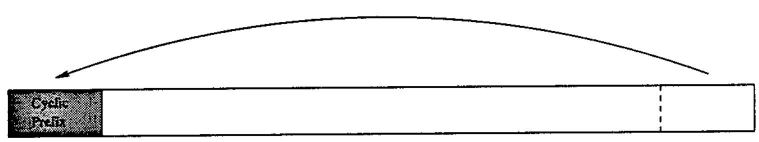

Figure 2.7: Adding the Cyclic Prefix

To handle multipath fading, cyclic prefix is generally combined with differential modulation scheme such as DPSK. Differential detection avoids the need for phase recovery, which can be difficult in a fast fading environment.

It is simple to implement, and when used in conjunction with a cyclic prefix, removes ICI and ISI without the need for adaptive equalization and training sequences. The disadvantage is that DPSK suffers about a 3 dB penalty compared to coherent demodulation. In DPSK, the information is carried by the change in phase between two symbols, rather than the absolute phase. It assumes that the channel does not change significantly over the two symbols, and will perform the same phase rotation on both symbols. Thus, the difference in phase will remain unchanged after passing through the channel, even if the actual phase rotation is unknown. With OFDM, bits can either be differentially encoded between bins on the same FFT block, or between consecutive blocks using the same bin.

Equalization can be used instead of differential detection in conjuction with the cyclic prefix. In this case, coherent detection can be performed and the performance loss due to differential detection is removed.

The following is a brief overview of equalization techniques for OFDM signals. As already noted, the OFDM modulator and demodulator can be implemented using an IDFT and DFT, respectively. Samples of the OFDM signal, generated by IDFT can be represented as

$$x(n) = \sum_{k=0}^{N-1} X(j,k) e^{i2\pi kn/N}, \tag{2.13}$$

where k refers to subcarrier order, j is time index and n is the sample number of the OFDM symbol. N is the length of the IDFT which is also the total number of subcarriers. When samples $x(n)$ are directed through a linear channel, $h(n)$, with additive noise $d(n)$, the received samples, $y(n)$ is,

$$y(n) = x(n) * h(n) + d(n). \tag{2.14}$$

The receiver demodulates the received samples using a DFT. From (2.14) the signal can be expressed in the frequency domain as

$$Y(k) = X(k)H(k) + D(k). \tag{2.15}$$

Depending on the channel, the received and demodulated signal samples are more or less distorted, i.e. $Y(k) \neq X(k)$. An equalization function $W(k)$ can be introduced to compensate the channel effects.

$$\hat{X}(k) = W(k)Y(k) = W(k)X(k)H(k) + W(k)D(k). \qquad (2.16)$$

The compensation coefficients of $W(k)$ can be generated using a conventional LMS algorithm and using a decision-directed structure, as illustrated in Figure 2.8. The adaptive algorithm operates independently for each of the

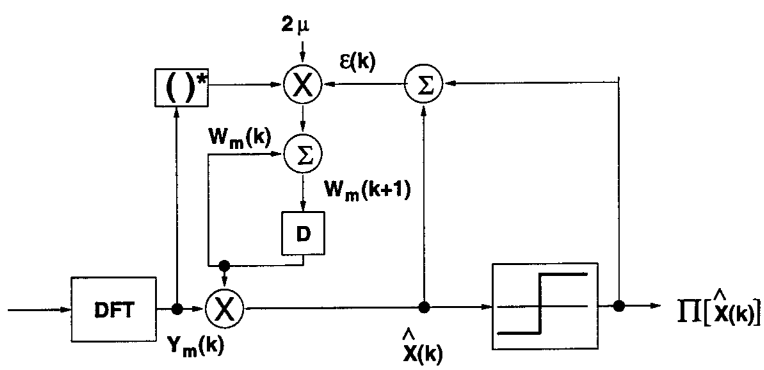

Figure 2.8: Conventional Least-Mean-Squared (LMS) equalizer

individual subcarriers and is governed by,

$$\hat{X}(k) = W_m(k)Y_m(k), \qquad (2.17)$$

where

$$\epsilon(k) = \hat{X}(k) - \Pi[\hat{X}(k)] \qquad (2.18)$$

and

$$W_m(k+1) = W_m(k) + 2\mu\epsilon(k)Y_m^*(k). \qquad (2.19)$$

The same approach can be used for spread spectrum OFDM except that the decision is made based on a decision variable found by coherently combining the energy from all the carriers. As a result, instead of working on a

subcarrier-by-subcarrier basis adaptation, the algorithm treats all the subcarriers as a group and the adaptation is governed by,

$$\hat{X}(k) = \sum_{m=0}^{N-1} W_m(k) Y_m(k), \tag{2.20}$$

where,

$$\epsilon(k) = \hat{X}(k) - \Pi[\hat{X}(k)], \tag{2.21}$$

and

$$W_m(k+1) = W_m(k) + 2\mu\epsilon(k) Y_m^*(k). \tag{2.22}$$

The conventional LMS algorithm is well suited for static or time invariant conditions due to its slow convergence behavior. The dynamic channel and interference conditions of the tactical PRN will require faster converging algorithms [24, 25].

2.2.4 Rate Adaptive Schemes

To operate with a channel of variable quality, it is necessary to either design the signal for the worst-case or make the signal adaptive. The non-adaptive case is wasteful of system resources, i.e. bandwidth and/or power, since the worst-case conditions will occur only a small fraction of the time. Adaptation can take many forms, including adjustment of the transmit signal power and changes in the signaling rate. Although transmission power control is a basic technique to compensate for the received signal loss due to fading, it tends to conflict with the LPI/LPD requirement for the tactical networks.

The most primitive adaptive modulation was first proposed by Cavers as an alternative to the power control technique in a Rayleigh faded channel [26]. In this case, symbol rate is adaptively controlled according to the received signal level. However, it requires very complicated hardware to generate various clock rates as well as to prepare transmitter and receiver filters matched to the possible bit rates.

Another possible modulation parameter for adaptive modulation is the number of constellation levels. Hanzo proposed a modulation level controlled adaptive modulation using variable QAM [27]. The system has much lower hardware complexity than the symbol rate controlled systems because the same modem configuration can be employed for any number of modulation levels. The concept of trading off user data rate with bit error performance can be applied to both single-carrier and multi-carrier systems. Hanzo [28], Goldsmith [29, 30], Sampei [31], Kalet [32], Czylwik [33], Wittke [34] and Cioffi [35] have studied adaptive modulation for either the single carrier or multi-carrier systems. Figure 2.9 illustrates the adaptive modulation concept. Instead designing for the worst case situation, e.g. the fringe of the coverage region in an AWGN channel, as in a fixed rate system, the adaptive system varies its number of constellation levels according to the channel quality, resulting in better utilization of the network resources.

OFDM is a bandwidth efficient multicarrier modulation scheme because it allows the subcarriers to overlap spectrally. There has been considerable effort to optimize the bandwidth utilization by studying the loading algorithm uses to assign transmit bits to the individual subcarriers. The adaptive modulators select from different QAM modulation formats, e.g. no modulation, 2-PSK, 4-PSK, 8-QAM, 16-QAM, 32-QAM, 64-QAM, 128-QAM and 256-QAM based on the channel SNR conditions. This means that 0, 1, 2, 3, ...8 bits per carrier or per subcarrier can be transmitted. In each case the constellation size of each individual carrier is adjusted independently in accordance with the signal quality in its particular channel.

Most of the adaptive modulation schemes studied to date are oriented toward a channel with a reasonably high signal-to-noise ratio (SNR). In these systems, the users all agree to shutdown transmission when the channel SNR falls below some threshold. We propose to study the throughput optimization problem in a low channel SNR dominant situation. Such a

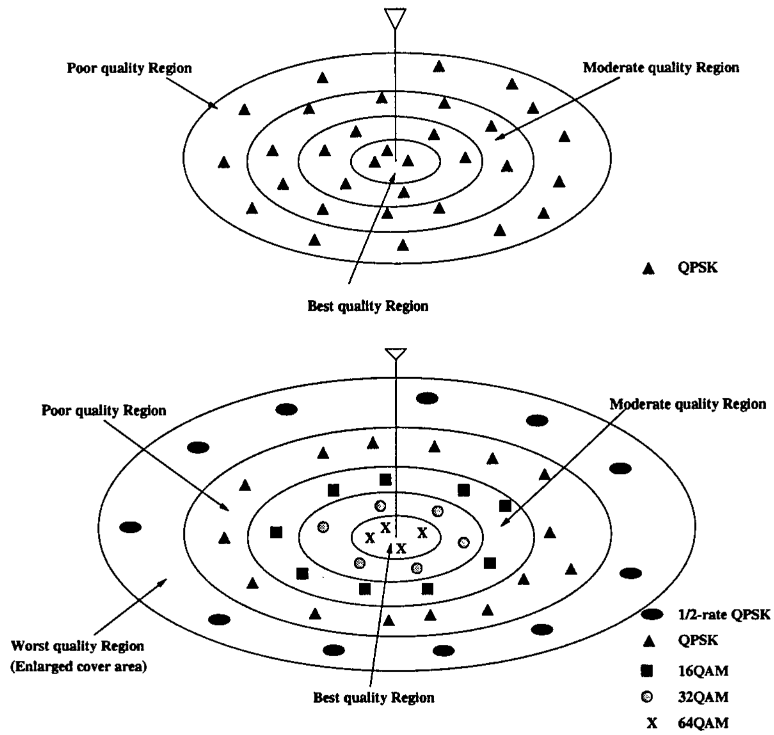

Figure 2.9: Fixed rate system vs. adaptive system with variable constellation

scenario prevails in military tactical networks where the channel is mostly under jammer control and it also appears in commercial wireless networks when mobiles are wandering in the cell coverage fringe areas. Other potential applications exist, such as the power limited space and satellite communications. Our adaptive rate scheme builds upon OFDM-SS [21, 36] and, instead of shutting down transmission at these poor SNR areas, it increases the processing, thereby allowing the receiver to boost the despread SNR through coherent combining of subcarrier energy.

2.3 Wireless Networks

2.3.1 802.11

We are all being exposed to a communications revolution that is taking us from a world where the dominant mode of electronic communications was standard telephone service and voiceband data communications carried over fixed telephone networks, packet-switched data networks, and high-speed local area networks to one where a tetherless and mobile communications environment has become a reality.

Wireless networks can be categorized into voice-oriented and data-oriented networks. The focus of this report is on data-oriented packet radio networks, generally called wireless LANs (WLAN). WLANs are designed for local high speed wireless communication among communication terminals. Its concept was first introduced around 1980 [37, 38]. In the middle of that decade, the ISM bands were released in the US [39, 40] for communications use. The first WLAN products appeared in the market around 1990 [41, 42, 43] and IEEE 802.11 standards work started shortly after that [44, 45]. Today, a variety of technologies and several sectors of the market have been examined for WLANs, and major international standards are evolving.

The IEEE 802.11 committee and the European Telecommunications Standard Institute (ETSI) RES-10 committee for HIPERLAN are developing standards for physical and MAC layers of WLANs. IEEE 802.11 is focusing on operation in the ISM bands and are restricted to spread spectrum technology. For the 900MHz and 2.4GHz bands, WLANs use either direct sequence spread spectrum (DSSS) or frequency hopping spread spectrum (FHSS). Because of the advantages of OFDM, IEEE 802.11 standard committee has adopted OFDM as the modulation scheme for the 5GHz band and OFDM is also targeted to be a common physical layer specification for the worldwide band for license exempted devices. The ETSI's RES-10 consid-

ered decision feedback equalization (DFE), multicarrier modulation (MCM) and sectored antenna systems (SAS) for the HIPERLAN, finally deciding on DFE. MCM was not adopted for the HIPERLAN, presumably because of the need for highly linear RF amplifiers which are difficult to build with the limited power available for PCMCIA add-ons. However, the area of minimizing peak-to-average power ratio is currently very active and it is believed that solutions to this problem will become available to avoid using highly linear RF amplifiers for the OFDM systems.

DSSS is one of the adopted modulation techniques in the current IEEE 802.11 standard, though it is not used used with CDMA, but rather, with Carrier Sense Multiple Access with Collision Detect (CSMA/CD). For the 2.4 GHz ISM band, the available bandwidth is 83.5 MHz. Most of the current implementations of 802.11 use an 11-chip Barker code as the spreading sequence, providing only a small amount of processing gain. For a 1 MHz data rate with binary phase shift keying (BPSK) or a 2 MHz rate with quaternary PSK (QPSK), the single channel bandwidth is approximately 22 MHz. The combination of signal and available bandwidth translates to three independent channels in the 2.4 GHz ISM band. Actual implementations specify 8 partially overlapping channels in the band and force a given network to use only one of the channels. Multiple channels are used to provide the capability for multiple co-existing networks.

The performance of DSSS in fading channel is generally good if the bandwidth of the spread signal is substantially greater than the coherence bandwidth of the channel. The use of a RAKE [3] receiver structure further enhances the performance. One drawback of the DSSS/CDMA signaling is that it may have difficulty operating in a mesh network, i.e. one supporting peer-to-peer communication. The reason for the concern is that DSSS/CDMA operates best with power control which minimizes or, ideally, eliminates, the near-far problem. Imprecise power control greatly diminishes the capacity

of a DSSS/CDMA network by increasing the multi-user interference. Power control is best utilized in a star network where all users are communication with a central station which provides the power control information which makes all the signals arrive at the same power level. Within a mesh network, the varying distances between communicators makes effective power control at best very complicated and, more likely, impossible. DSSS has been thought to be only for low- or medium-bit-rate transmission like kilobit-per-second transmissions in some cellular systems and megabit-per-second transmissions in ISM bands, since it requires much wider radio bandwidth than data bandwidth. Assuming 156 Mb/s for asynchronous transfer mode (ATM) transmission in a submillimeter- or millimeter-wave band, SS transmission with Gp (processing gain) = 15 requires 2.325 GHz. Such broad bandwidth does not seem realistic for a simple direct sequence (DS) method for the following two reasons:

- Severe interchip interference occurs.
- It is difficult to synchronize such a fast sequence at a receiver.

Frequency hopping is another adopted modulation technique for the IEEE 802.11 standard. There are many variations of frequency hopping which may be valuable for a channel with multipath fading and jamming. In one case, the hopped carrier is a narrowband signal, such as a frequency-shift keyed (FSK) signal. Fast frequency hopping, in which one symbol is spread over multiple hops, and slow hopping in which one or more symbols are transmitted at each hop frequency provide the frequency diversity needed to combat multipath and narrowband interference.

In summary, all techniques have advantages and disadvantages. Direct sequence has the advantage that processing gain (data rate) can be easily varied but has the disadvantage of occupying the entire bandwidth, leaving the receiver open to interference within any portion of the band. Frequency

hopping has the interference avoidance capability but it can be more difficult to vary the data rate over a wide range. On the contrast, multicarrier modulation, OFDM in particular, is a technique which has some of the advantages of both direct sequence and frequency hopping. In this technique, multiple carriers are used to send the message and, depending on how the carriers are used, the resulting signal can be made to look similar to a direct sequence signal or a frequency hopping signal. A major advantage is that it is possible to easily and rapidly change the signal characteristics, including the processing gain. It is for this reason that there is considerable research activity oriented toward using OFDM for the new generation wireless network standards.

Chapter 3

The RA-OFDM System

3.1 Introduction

Orthogonal frequency division multiplexing (OFDM) [14, 17] has received considerable attention as a method to efficiently utilize channels with non-flat frequency responses and/or non-white noise. In its most common form, a high rate data stream is divided up among the many carriers in the system in a manner which optimizes the capacity of the overall channel. OFDM can also be used as a spread spectrum modulation (OFDM-SS) [18, 19, 20, 21] wherein spectral spreading is accomplished by putting the *same data* on all the carriers, producing a spreading factor equal to the number of carriers. At the receiver, the energy from all the carriers is coherently combined to produce the decision variable. Multiple users can be supported in the same channel through Code Division Multiple Access (CDMA) [22]. In this case each user has a unique signature sequence which determines the set of carrier phases. To receive a particular signal, the receiver needs to know the signature sequence for that user in order to align the carrier phases for the coherent combining operation.

The use of spreading with OFDM provides anti-jam capability as well as

enabling the use of CDMA. While resistance to jamming is clearly important in a tactical network, the use of spreading tends to limit the available throughput due to the bandwidth expansion. A main focus of this chapter is the study of the performance of an OFDM system which makes it possible to vary the data throughput in response to channel conditions. When anti-jam capability is needed, the signaling format is adjusted to increase the spreading while, when the channel is clear, spreading is reduced to increase the throughput. More specifically, in a favorable channel, the system would operate much like the conventional OFDM system where different data bits are transmitted on different carriers yielding high throughput. In a severe interference channel, the system would operate like the OFDM-SS system, sacrificing throughput to provide the needed processing gain to overcome the jamming. In most cases, the system would operate between these two extremes, providing sufficient processing gain to mitigate the channel effects while maximizing throughput. We call this system rate-adaptive OFDM (RA-OFDM). Figures 3.1 and 3.2 compare the conventional OFDM system with a RA-OFDM system.

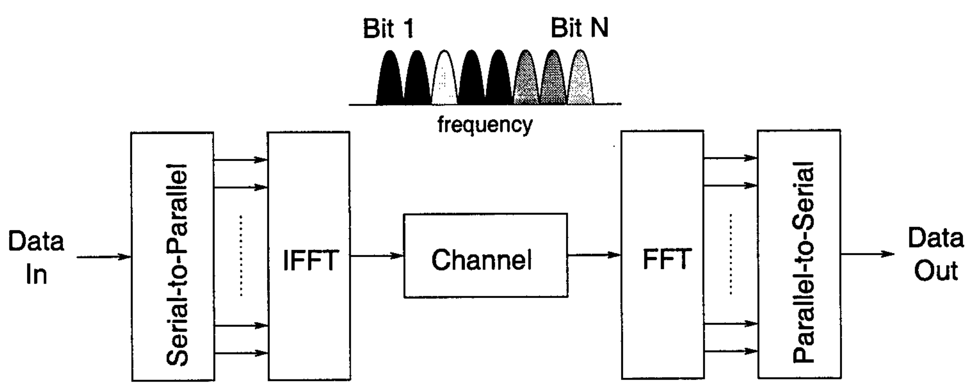

Figure 3.1: Conventional OFDM System

The ultimate goal for the RA-OFDM system is to provide reliable com-

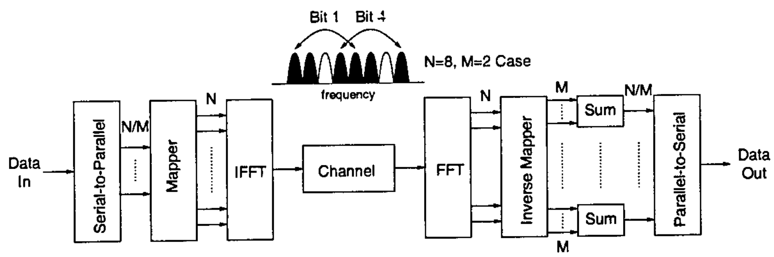

Figure 3.2: Variable Processing Gain OFDM

munications over a broad range of channel conditions through the adjustment of the processing gain. Additive white Gaussian noise (AWGN), frequency-selective Rayleigh fading and flat Rayleigh fading channels will all be considered and the emphasis is on developing a single adaptive strategy that will apply in all cases. The focus of this chapter, then, is to demonstrate the effectiveness of the RA-OFDM concept for each of the channel types and to show that the adaptation scheme is of reasonable complexity.

Adaptivity of the proposed system stems from the easy manipulation of the system processing gain. To allow an efficient application in a packet radio network, the system should introduce minimum overhead for equalizer training, especially upon rate adaptation. In the following sections, we present the RA-OFDM system which allows a smooth transition of processing gain to track the changing channel conditions. Its use in a packet radio network environment is discussed and simulation models are introduced. The performance of the RA-OFDM system under AWGN, static multipath, frequency selective fading and frequency-nonselective fading channels completely justifies the rate adaptation concept. The chapter concludes with an overall system adaptation strategy which allows reliable communications in a broad range of channel conditions, including AWGN, frequency-selective fading, flat fading and interference.

3.2 RA-OFDM Receiver

With OFDM modulation, variable throughput can be implemented by changing the amount of redundancy in the placement of data bits on the carriers. For simplicity, assume initially that the data is not coded. The highest throughput is accomplished by sending different data on each of the carriers. This arrangement does not provide significant anti-jam capability nor does it produce any frequency diversity to help mitigate the effects of frequency selective fading. Inserting a processing gain of 2 requires that the same data be sent on a pair of carriers, preferably spaced apart in frequency to produce frequency diversity for both multipath and anti-jam protection. Increasing the processing gain to 4 requires sending the same data on 4 carriers, a processing gain of 8 requires sending the same data on 8 carriers, etc. The maximum processing gain available equals the number of subcarriers in the system.

In order to make the format adaptive, i.e. make the processing gain respond to channel conditions, it is necessary to assume that the receiver will feedback some information to the transmitter. This feedback is necessary because it cannot generally be assumed that the transmitter knows the channel as seen by the receiver. Additionally, any changes made to the transmit signal format must be accommodated by the receiver, meaning that the receiver must adapt its demodulation and detection operations to adjust to the changes in the signal. The information that is returned can take many forms, from a simple received signal quality measurement to detailed information on the properties of the interference. For instance, if a fixed-frequency narrowband jammer is present, the receiver may feed this information back to the transmitter which can then avoid the use of carriers in the jammed frequency band, shifting the transmit power to other carriers. In this chapter, we will only consider the simplest case, where the transmitter changes the

processing gain of the transmitted signal on a packet-by-packet basis and the receiver learns of these changes through the packet preamble. An example packet structure will be provided later.

Multipath fading induces phase and amplitude variations in the subcarriers. For flat fading, these variations are the same for all the carriers while for frequency selective fading the variations are different for each carrier. There are two common ways of dealing with the effects of this fading: differential detection and equalization. With flat fading, differential detection can be performed after the energy from the carriers is combined, since the fading is the same for all carriers. In the more general frequency selective fading case, however, differential detection must be performed individually on each carrier before the combining operation. Since the signal-to-noise ratio on the individual carriers is low when the processing gain is large, the losses due to differential detection can be quite large in this case. In this chapter, we will consider a receiver that uses equalization [46, 47] instead of differential detection. While the equalizer can provide better performance, it may have difficulty tracking rapidly changing fading or interference.

Figure 3.3 shows the RA-OFDM receiver which uses an equalizer to compensate for channel effects. In the diagram, each summer has M inputs (processing gain is M) and K symbols are sent simultaneously. M and K will vary depending on the processing gain requirements but the product MK will always equal the number of carriers. We have studied various frequency domain adaptive equalizer structures in [21, 48]. Here we choose the simplest one dimensional structure with only one layer of forward taps to equalize the channel. Since simplicity is the utmost requirement for the whole adaptive structure, it is coupled with the conventional cyclical prefix approach [3, 49] to handle ISI and ICI mitigation. It is important that the equalizer coefficients not need to be re-trained as a result of a change in processing gain. The reason for this is that one possible operation scheme

involves training the equalizer at the highest processing gain using a packet preamble and then changing the processing gain for the packet payload. This is discussed in more detail in the next section. Since each complex equalizer coefficient has a value that is a function of the *channel*, it is not dependent on the spreading scheme and it is possible to have glitch-free switching between processing gains.

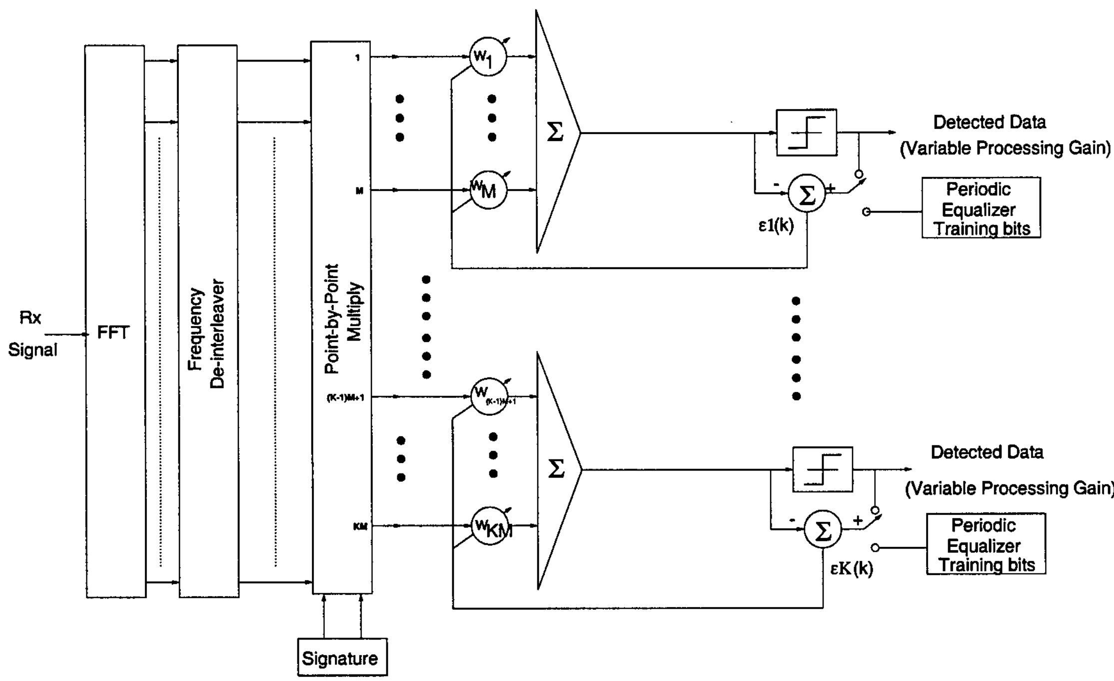

Figure 3.3: Block Diagram of a RA-OFDM receiver with glitch-free switching between processing gain. Here the processing gain is M and K symbols are sent simultaneously.

3.3 Contrast with other Rate Adaptive Approach

In the following, we use an information theoretic approach to compare and contrast our proposed RA-OFDM system with the adaptive modulation techniques based on variable QAM. We will not only establish the similarity between the techniques, but also point out the advantages of our scheme as an unifying modulation across a wide range of channel conditions.

The problem of optimizing channel capacity dates back to the 40's [50, 51, 52]. In the past decade, with the ever increasing need to provide very high speed data communication over landline telephone network or wireless media, this problem has received increased emphasis. Chapter 2 provided an overview of many of the adaptive modulation techniques that have been proposed.

3.3.1 Channel Capacity, AWGN Channel, High SNR

The multicarrier modulation system under consideration is shown in Figure 3.4. Throughout the analysis, we will use the following notation:

- $H(f)$: channel frequency transfer characteristic
- W: total bandwidth of the multicarrier system
- N: total number of subcarriers of the multi-carrier system
- $N_0/2$: spectral density of additive white gaussian noise
- P_{av}: average transmitted power

Recall that the capacity of an ideal, band-limited, AWGN channel is:

$$C = W \log_2 \left[1 + \frac{P_{av}}{WN_0}\right] \tag{3.1}$$

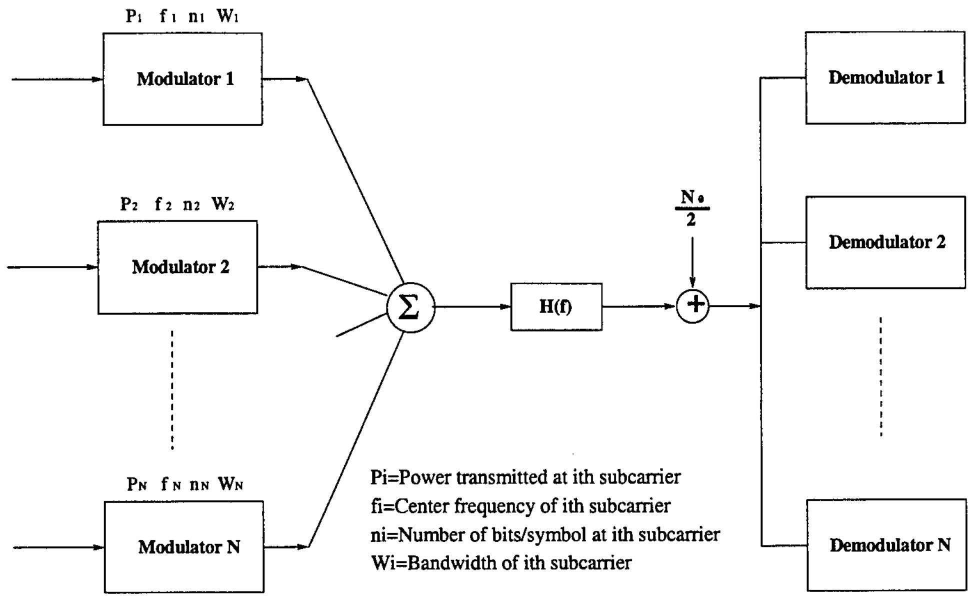

Figure 3.4: The multicarrier modulation system

where C is the capacity in bits/s. Consider a multicarrier system with a large number of carriers spaced Δf apart. If the total bandwidth is held fixed at W, the carrier spacing will go to zero in the limiting case as the number of carriers goes to infinity. In this system, the transmitted power P is divided into the very large number of subcarriers, each one with power $\Delta f P k(f)$, in which $k(f)$ is the normalized power distribution. Each subchannel has capacity:

$$C_i = \Delta f \log_2 \left[1 + \frac{\Delta f P}{N_0 \Delta f} k(f) \left|H(f)\right|^2\right] = \Delta f \log_2 \left[1 + \frac{P}{N_0} k(f) \left|H(f)\right|^2\right] \tag{3.2}$$

and the bit rate becomes

$$R_b = \int_{f \in W} \log_2 \left[1 + \frac{P}{N_0} k(f) \left|H(f)\right|^2\right] df. \tag{3.3}$$

The optimized power distribution $k_{opt}(f)$ is found to be

$$k_{opt}(f) = \lambda - \frac{1}{K_0 \left|H(f)\right|^2} \tag{3.4}$$

where

$$\int_{f \in W} k_{opt}(f) df = 1$$
$$K_0 = \frac{P}{N_0}$$

and λ is a Lagrange multiplier. The maximum bit rate, R_{bmax} is given by

$$R_{bmax} = \int_{f \in W} \log_2(\lambda K_0 \left|H(f)\right|^2) df. \tag{3.5}$$

This expression of the channel capacity of a linear filter channel with additive Gaussian noise is due to Shannon. The basic interpretation of this result is that the signal power should be high when the channel SNR is high, and low when the SNR is low. This result is the so-called *water-filling interpretation* of the optimum power distribution as a function of frequency.

Now, apply the Lagrange multiplier method to the case where QAM modulation is used on the subcarriers. The transmitted signal consists of N QAM carriers, each with a rectangular Nyquist spectrum of bandwidth equal of W_i Hz. In the limit as $W_i \to 0$, we have an "infinite" multitone QAM signal. Start with a relatively high channel SNR assumption so that we can use a high level constellation size. According to Kalet [32], the bit rate R_b is given by:

$$R_b = \int_{f \in W} \log_2 \left[1 + \frac{3}{\left[Q^{-1}\left(\frac{P_e}{K}\right)\right]^2} \frac{P}{N_0} k(f) \left|H(f)\right|^2 \right] df, \tag{3.6}$$

where P_e is the desired BER. K is a real constant such that $2 \leq K \leq 4$ and it is dependent on the constellation size, i.e. number of bits/symbol. R_b can

be tightly upper or lower bounded by choosing K equal to two or four. The forward Q function is defined by

$$Q(x) = \frac{1}{\sqrt{2\pi}} \int_x^\infty e^{-y^2/2} dy.$$

The optimized power distribution $k_{opt}(f)$ is found to be

$$k_{opt}(f) = \lambda - \frac{1}{K_1 |H(f)|^2}, \tag{3.7}$$

where

$$\int_{f\in W} k_{opt}(f) df = 1$$

$$K_1 = \frac{P}{N_0} \frac{3}{\left[Q^{-1}\left(\frac{P_e}{K}\right)\right]^2}$$

and λ is a Lagrange multiplier. The maximum bit rate, R_{bmax} is given by

$$R_{bmax} = \int_{f\in W} \log_2(\lambda K_1 |H(f)|^2) df. \tag{3.8}$$

If we compare (3.5) and (3.8), we have essentially shown that, independent of the shape of $|H(f)|^2$, the degradation of the "infinite" multitone signal to the capacity of any $|H(f)|^2$ is the same and the degradation is solely dependent on the factor $\frac{3}{\left[Q^{-1}\left(\frac{P_e}{K}\right)\right]^2}$, i.e. the desired BER and modulation constellation size. Let's verify this with an example of a flat channel response. In this case, $|H(f)| = H$ and the optimum power distribution is

$$k_{opt}(f) = \lambda - \frac{1}{K_1 |H|^2} = \frac{1}{W}$$

$$\int_{f\in W} k_{opt}(f) df = W * k_{opt}(f) = 1$$

and the optimum bit rate is

$$\begin{aligned}
R_{bmax} &= \int_{f\in W} \log_2(\lambda K_1 |H|^2) df = \int_{f\in W} \log_2 \left[\left(\frac{1}{K_1 H^2} + \frac{1}{W}\right) K_1 H^2\right] df \\
&= \int_{f\in W} \log_2 \left[1 + \frac{K_1 H^2}{W}\right] df \\
&= W \log_2 \left[1 + \frac{K_1 H^2}{W}\right] = W \log_2 \left[1 + \frac{P}{N_0} \frac{3}{\left[Q^{-1}\left(\frac{P_e}{K}\right)\right]^2} \frac{H^2}{W}\right] \\
&= W \log_2 \left[1 + \frac{P H^2}{W N_0} \frac{3}{\left[Q^{-1}\left(\frac{P_e}{K}\right)\right]^2}\right] \qquad (3.9)
\end{aligned}$$

PH^2 is just the average power P_{av}, therefore,

$$R_{bmax} = W \log_2 \left[1 + \frac{P_{av}}{W N_0} \frac{3}{\left[Q^{-1}\left(\frac{P_e}{K}\right)\right]^2}\right] \qquad (3.10)$$

Now the degradation compared to the Shannon capacity can be easily found. The basic formula for the capacity of the band-limited AWGN waveform channel with a band-limited and average power-limited input is

$$C = W \log_2 \left[1 + \frac{P_{av}}{W N_0}\right] \qquad (3.11)$$

so the degradation term is $\frac{3}{\left[Q^{-1}\left(\frac{P_e}{K}\right)\right]^2}$. For $P_r(\epsilon) = 10^{-5}$, there is about 8.4 dB degradation in performance when comparing "infinite" multitone to the Shannon capacity.

3.3.2 Channel Capacity, AWGN Channel, Low SNR

The adaptive QAM system works effectively in a high SNR situation. When the channel is dominated by low SNR, this variable QAM system will simply turn off transmission. We have taken a somewhat different approach to rate adaptation in a multi-carrier framework. Our proposed RA-OFDM scheme

continues to transmit even in the poor SNR situation and it strives to approach the channel capacity within a performance gap determined solely by the desired BER.

The RA-OFDM system is adaptive in that the amount of spreading, i.e. the number of redundant carriers, is varied in response to channel conditions. In addition to varying the number of redundant carriers, the constellation size can be varied on the carriers, allowing high level QAM such as 64-QAM, 128-QAM or 256-QAM to be used to produce even higher throughput in excellent channel conditions.

With BPSK and OFDM-SS modulation we have,

$$P_e = Q\left(\sqrt{2\frac{E_c}{N_0}P_g}\right), \tag{3.12}$$

where E_c and P_g are the chip energy and processing gain, respectively. Considering the overlapping nature of the multi-carriers, we find

$$R_b = \frac{W}{P_g} = W\frac{2\frac{E_c}{N_0}}{[Q^{-1}[P_e]]^2}. \tag{3.13}$$

When the channel is dominated by low SNR, $P_g \gg 1$, so $\frac{2\frac{E_c}{N_0}}{[Q^{-1}[P_e]]^2} \ll 1$. Use the approximation $x \simeq \log_2(1+x)$ when $|x| \ll 1$ to obtain

$$R_b \simeq W\log_2\left(1 + \frac{2\frac{E_c}{N_0}}{[Q^{-1}[P_e]]^2}\right).$$

Denote T_s as the symbol duration and N as the total number of subcarriers. With a little simplification we find

$$\frac{E_c}{N_0} = \frac{P_{av}T_s/N}{N_0} = \frac{P_{av}T_sW/N}{N_0W} = \frac{P_{av}}{WN_0} \tag{3.14}$$

and the bit rate becomes

$$R_b = W\log_2\left(1 + \frac{2\frac{P_{av}}{N_0W}}{[Q^{-1}[P_e]]^2}\right). \tag{3.15}$$

Following the same Lagrange multiplier method that was used earlier, the optimal throughput found to be,

$$R_b = \int_{f \in W} \log_2 \left[1 + \frac{2}{[Q^{-1}(P_e)]^2} \frac{P}{N_0} k(f) \left| H(f) \right|^2 \right] df. \qquad (3.16)$$

Comparing this result to the previous one for the multitone QAM system, there exists striking similarity between our proposed adaptive system and the multitone QAM system. The degradation factor now is $\frac{2}{[Q^{-1}(P_e)]^2}$ instead of $\frac{3}{[Q^{-1}(\frac{P_e}{K})]^2}$. Performance results for our system are shown in Figure 3.5. When the BER requirement is $P_b = 10^{-5}$ the performance gap between the adaptive processing gain system and the Shannon capacity is 9.59dB. When the BER requirement is reduced to $P_b = 10^{-3}$, the gap is reduced to 6.8dB. It is worth pointing out that our proposed system continues to deliver throughput at very low SNR while the multitone QAM system has to work in a much higher SNR region.

The BER of coherent M-QAM with two-dimensional Gray coding over an AWGN channel with perfect clock and carrier recovery can be approximated by [29]

$$BER \simeq 0.2 e^{-\frac{3\gamma}{2(M-1)}} \qquad (3.17)$$

in which γ is the SNR and M is the number of constellation points. Therefore, $M = 256$ for 256-QAM. Coupling this with a processing gain of 4, we have

$$BER \simeq 0.2 e^{-\frac{3\gamma}{2(256-1)} P_g} \simeq 0.2 e^{-\frac{3\gamma}{2(64-1)}} \qquad (3.18)$$

and we have essentially shown that a high level QAM with processing gain delivers the same BER performance as a system with lower level QAM without processing gain. If we can consider high level QAM as a special case of spread spectrum system in which the processing gain is less than one, we have a OFDM-SS system with variable processing gain across all channel SNR conditions. Variable processing gain becomes a universal way to implement adaptivity.

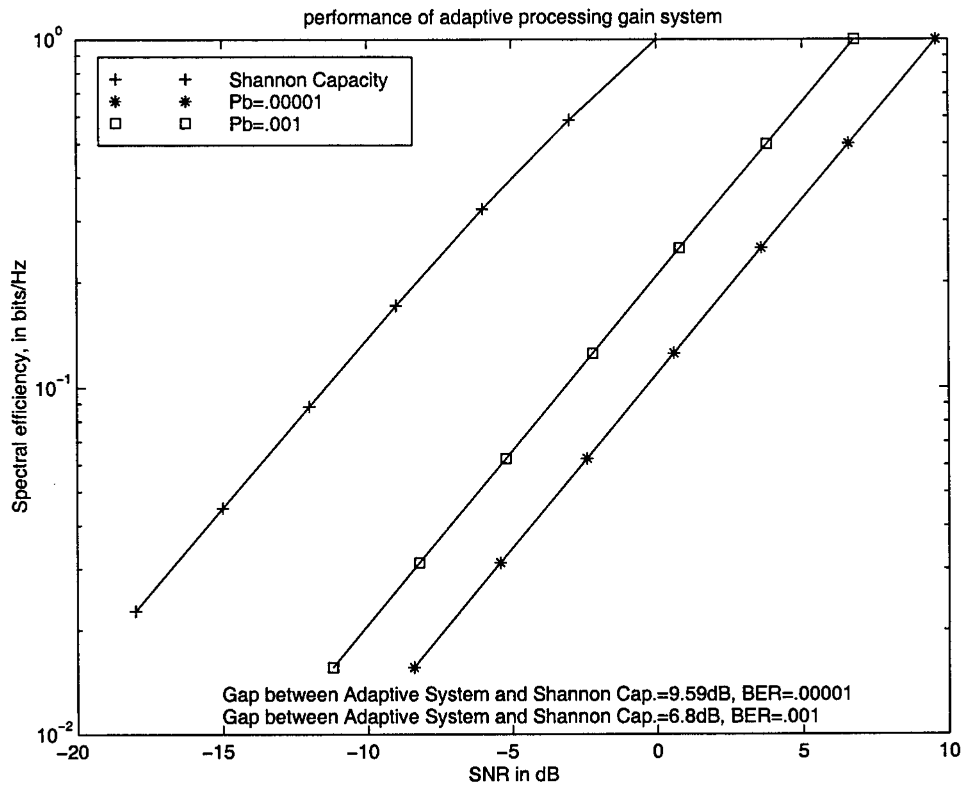

Figure 3.5: Throughput of adaptive processing gain system, at low SNR case

In summary, both the RA-OFDM system and the variable QAM system mitigate signal quality degradation using additional redundancy as a resource. In an AWGN or frequency non-selective channel, this redundancy translates into higher effective "SNR" for the received signal. Variable QAM is more often used in a wireline modem and operates on a higher SNR scale than the RA-OFDM system. Due to the large power fluctuations in a wireless channel, it is difficult to reliably demodulate signal sets with large numbers of points without using complex equalization approaches. In addition to this, the military applications generally require LPI/LPD. All of these means that

RA-OFDM system is more favorable in a tactical wireless application. Furthermore, as will become clearer in the later sections, RA-OFDM scheme not only boosts up the effective SNR seen by the receiver, but can also provide additional diversity gain in a frequency selective channel, an advantage that is not presented in other adaptive modulation schemes. It must be mentioned that one of the fundamental characteristics of a communication link is the possibility of a trade-off between bandwidth and power to obtain a specified received signal power quality. Our proposed modulation scheme is especially well suited for power limited links such as a mobile satellite system, while the variable QAM scheme is more appropriate for bandwidth limited links such as the landline modems.

3.4 Simulation Models

The RA-OFDM scheme is envisioned for use in a packet radio network. An example packet structure that has a fixed number (1280) of symbols as shown in Figure 3.6. The packet consists of unique words (UW) for periodic equalizer training (needed only for an equalizer-based receiver), data rate indicator, optional FEC for the rate indicator and actual data symbols transmitted. Except for the information symbols, all the other parts of the packet are transmitted using the maximum level of processing gain to ensure maximum error protection and to enable all receivers, including those with poor channels, to attain packet synchronization. In all cases, accuracy of the rate indicator is essential because received signal can not be correctly demodulated unless the modulation parameters are correctly decoded. The processing gain for the actual information bit stream depends on the channel conditions. Note that in this scheme, if the structure of the OFDM signal, i.e. the number of carriers and the carrier spacing remains unchanged, the duration of each packet will depend on the processing gain that is used, even

though the number of symbols is held constant.

The variable rate system can operate in either either time division duplex (TDD) or frequency division duplex (FDD) modes. With TDD, both base station (BS) and mobile station (MS) transmit over the same RF channel, but at different times. In this case both BS and MS experience similar channel fading conditions as their transmissions are typically half a TDD frame apart. The transmission received by the MS is used to estimate the channel integrity which then dictates the processing gain used by the MS transmitter. Similarly, the transmission received by the BS enables the processing gain levels used in the subsequent BS transmission to be determined. With FDD, the uplink and downlink use different RF frequencies typically spaced by more than the coherence bandwidth of the channel. Therefore the fading on the two links may differ substantially. Both the BS and MS must monitor their incoming channels and signal the required levels of processing gain by the other in their transmission on their outgoing channels.

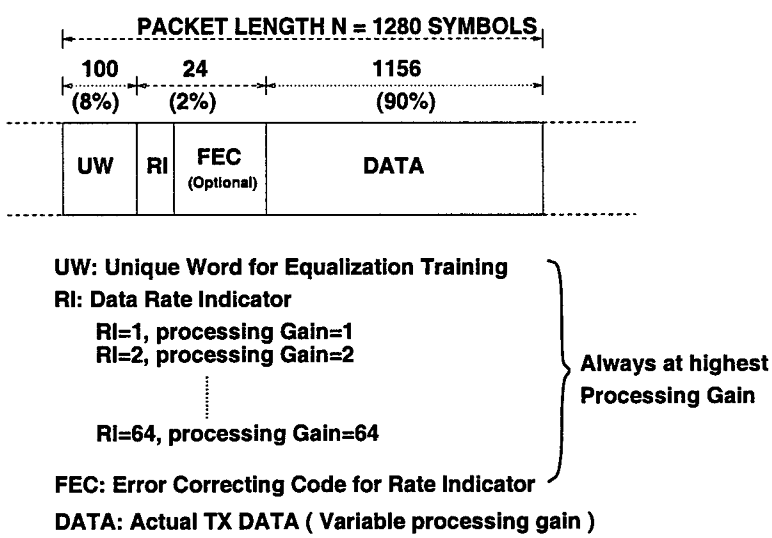

Figure 3.6: Signal frame format for the RA-OFDM system

There are two criteria that can be used to judge the quality of the channel by the receiver. One uses the Receive Signal Strength Indicator (RSSI) and the other uses Bit or Word error rate. Both methods take advantage of the fact that the fixed bit stream pattern for equalizer training are known by both the transmitter and receiver. For RSSI switching mode, the average magnitude of the baseband signal level over a frame provides an indication of the short term channel path loss. For BER switching mode, as its name implies, bit error rate is used as an indicator to the channel condition. Block diagram of these two switching system is shown in Figure 3.7 for a TDD application. A FDD system works in the same principle except a feedback path is needed from receiver to transmitter.

The RA-OFDM system will be studied both analytically and through simulation. The analytical model is used primarily to study the performance in AWGN and flat fading channels while the simulation is used to validate the analysis and to obtain performance results for the frequency-selective fading channel. In all cases, perfect carrier and symbol synchronization is assumed between the transmitter and receiver.

In the simulation, the RA-OFDM modulator with variable processing gain and variable-rate coding, a number of channel models, and the rate adaptive receiver are implemented and used to perform Monte Carlo simulations. The equalizer is adapted using either the conventional LMS algorithm in a decision-directed mode or using perfect channel information. This later condition is used to allow performance estimation without the introduction of performance degradation due to imperfect equalizer tracking of the channel. It also makes the result independent of the Doppler rate.

A number of different fading channels are considered analytically and implemented in the simulation. The time-invariant multipath channel consists of two equal-power rays with an inter-ray delay of 10 samples. The time-varying frequency-selective fading channel model consists of multiple rays

spaced at sample intervals, T_c, and having a flat (uniform) intensity profile, meaning that the mean power is the same for each of the rays. Each ray is independently Rayleigh faded with an adjustable Doppler rate. With this arrangement, an 8-ray channel will have a total delay spread of 8 samples, i.e. $8T_c$. The Rayleigh fading channel is modeled by an M-state Markov chain. This concept of a finite-state Markov channel emerged from the early work of Gilbert [53] and Elliott [54]. Wang extended the concept of the two-state Gilbert-Elliott channel into the finite-state Markov channel [55]. The channel model is shown in Figure 3.8, where S_i corresponds to the ith channel state. The channel is in S_i when the received SNR, γ, satisfies $\gamma_{i-1} \leq \gamma < \gamma_i$ for some constant γ_{i-1} and γ_i. With BPSK signaling, the average channel bit error probability for state i is

$$p[\text{error}|i] = \int_{\gamma_{i-1}}^{\gamma_i} Q(\sqrt{2\gamma}) f(\gamma|i) d\gamma. \tag{3.19}$$

$f(\gamma|i)$ is the conditional distribution of γ given the channel is in state i and it is given by

$$f(\gamma|i) = \frac{\frac{1}{\gamma_0} e^{-\frac{\gamma}{\gamma_0}}}{e^{-\gamma_{i-1}/\gamma_0} - e^{-\gamma_i/\gamma_0}}, \tag{3.20}$$

where γ_0 is the average SNR. Consider a system which transmits at a rate of R_t symbols per second. The average transmission rate for state S_i is

$$R_t^i = R_t * \pi_i \tag{3.21}$$

symbols per second, where π_i is the probability that the channel is in state i. According to [55], the average rate at which the received SNR passes downward across the threshold γ_i is

$$N_i = \sqrt{\frac{2\pi\gamma_i}{\gamma_0}} f_d e^{-\frac{\gamma_i}{\gamma_0}}, \tag{3.22}$$

where f_d is the Doppler frequency. The Markov transitional probabilities are then approximated by

$$P_{i,i+1} \simeq \frac{N_i}{R_t^i} \quad i = 1, 2, ... M-1 \tag{3.23}$$

$$
\begin{aligned}
P_{i,i-1} &\simeq \frac{N_{i-1}}{R_t^i} \;\; i = 2, 3, ...M \;\; \text{and} \\
P_{1,1} &= 1 - P_{1,2}, \quad P_{M,M} = 1 - P_{M,M-1} \\
P_{i,i} &= 1 - P_{i,i-1} - P_{i,i+1} \;\; i = 2, 3, ...M - 1
\end{aligned}
\tag{3.24}
$$

For the RA-OFDM system, the transmission rate at each state is different due to the different processing gains. Therefore, R_t^i in (3.23) and (3.24) should be further normalized with the actual bandwidth expansion factor for that state. This Markov chain model is used to analyze the BER performance and throughput of the RA-OFDM system. Various numbers of states are used for the Markov chain.

Unless otherwise specified, the RA-OFDM signal consists of 64 carriers, the FFT in the receiver has 64 bins and perfect symbol synchronization is assumed, i.e. the blocks of the data processed by the FFT are time aligned with the symbol intervals of the non-delayed path. Similarly, all processing is performed at baseband, effectively assuming perfect carrier synchronization. Random data is sent by the transmitter and binary signaling is used. For the simulation, a minimum of 100 bit errors were recorded for each of the data points and sufficient time was allowed for the equalizer to converge before data collection began.

3.5 Results

3.5.1 AWGN and Time-Invariant Multipath Channel

We start by demonstrating the idea of rate adaptation using AWGN and static two-ray channels. The two-ray channel model has inter-ray delay of 10 samples. Theoretical BER results for AWGN and simulation BER results for the time-invariant two ray channel are shown in Figure 3.9. This figure illustrates that, as the received SNR (i.e. the SNR before despreading)

varies from -12 dB to 12 dB, a bit error rate of 10^{-3} can be maintained by appropriate control of the processing gain over a 24 dB range. Since the number of carriers remains fixed at 64 and the carrier spacing is unchanged, the throughput is being reduced each time the processing gain is increased. Most of the degradation from the AWGN performance that is evident in the multipath results is due to the fact that some of the channels are faded in the later case. Note that the larger the processing gain, the smaller this degradation due to the averaging effect of the despreading operation.

To test the actual rate adaptation scheme, we set up a dual rate system in a packet radio network environment. Using the packet frame structure we proposed earlier, 10 percent of each packet frame is dedicated to equalizer training. In this scenario, the "good" channel always enjoys a 3dB SNR advantage over the "poor" channel. In order to make up the SNR difference, we use twice the processing gain for the "poor" channel as for the "good" channel. The training is always performed with the maximum processing gain and, in the "good" channel case, the processing gain is decreased during the data transmission. The equalizer switches to decision directed mode during the message portion of the packet. Figure 3.10 plots the system performance under both channels as well as the BPSK theoretical results. Keep in mind that E_b/N_0 includes the benefit of the processing gain. As expected, the system achieves very similar performance under the different channels, which are both very close to the BPSK theory.

3.5.2 Rate Adaptation over Time-Varying Frequency Selective Fading Channels

The frequency-selective fading channel can provide a diversity gain because different portions of the frequency spectrum fade independently. The achievable diversity D depends on the transmission bandwidth B and the coherence

bandwidth $(\Delta f)_c$ and can be estimated roughly by [3],

$$D \approx B/(\Delta f)_c \tag{3.25}$$

The total number of carriers is fixed at 64 and we use a deterministic frequency interleaver which, if possible, separates the redundantly transmitted bits by the coherence bandwidth $(\Delta f)_c$. Thus, the maximum amount of frequency diversity is achieved. To concentrate on an accurate assessment of diversity gain, we will use perfect channel information to determine the equalizer coefficients as opposed to using an adaptive algorithm.

Figures 3.11 and 3.12 show the simulated BER versus E_b/N_0 for 4-ray and 8-ray channels, respectively. In each case, the processing gain (spreading factor) takes the values 1, 2, 4, 8, 16, 32 to 64 and coding is not used. Note that the power of the AWGN scales with changes in the processing gain. For a 4-ray channel, the achievable diversity as defined by (3.25) is 4. This fact is demonstrated in Figure 3.11 in which the BER performance improves with increased processing gain until $Pg = 4$, at which point no further gains are evident. The same conclusion holds true for the 8-ray model in Figure 3.12 in which the performance improves until $Pg = 8$. Therefore, for a typical mobile radio environment, the attainable diversity gain is limited by the coherence bandwidth and overall bandwidth of the channel. Matching the processing gain to the available diversity provides the best performance; spreading further beyond this point does not provide additional *diversity gain* but does still provide additional SNR gain. This latter point is evident if BER is plotted against received SNR rather than E_b/N_0.

To further demonstrate that diversity gain is a major contribution to the performance gains attained with larger processing gain, the theoretical performance curves for a diversity receiver using maximal-ratio combining are shown in Figure 3.13 [3]. The number of independent Rayleigh fading channels is denoted by $D = 1, 2, 4, 8$. Also shown are the simulation performance

results for the RA-OFDM receiver with 1-ray, 2-ray, 4-ray and 8-ray channels and when the processing gain matched to the channel, i.e. the processing gain is set to the lowest value which fully takes advantage of the frequency diversity. The simulation data matches the theoretical curve very well for $L \leq 4$ because, in these cases, the L carriers for each bit undergo independent Rayleigh fading. The simulation results do have a slight loss due to energy loss for the cyclical prefix. For $L = 8$ the gap between the simulation and ideal curve is larger, indicating that as the frequency spacing between carriers carrying the same information bit gets smaller, the Rayleigh fading becomes more statistically dependent, resulting in some loss in diversity gain.

3.5.3 Rate Adaptation over Frequency Non-selective Rayleigh Fading Channels

With flat Rayleigh fading, the channel frequency response at any given instant is flat across all the subchannels, meaning that diversity gain is not available by simply spreading, interleaving and/or coding across the carriers. Instead, time diversity must be obtained by using these techniques over blocks of data that span many symbol intervals, i.e. many FFT blocks. The slower the fading, the greater the needed time diversity and the less practical this solution becomes. For example, consider a slow fading channel characterized by 50Hz of Doppler frequency, yielding a coherence time, $(\Delta t)_c$, of $\simeq 0.02$s. If the sampling rate equals 1MHz and FFT block size is 64, achieving a two-fold diversity (in the time domain) requires an interleaver having the size of $2 \times .02/1 \times 10^{-6} = 40,000$ bits. In addition to the obvious storage and complexity problems, the total delay resulting from the interleaver/de-interleaver pair is 0.08s, a value that is much too high for most packet radio network applications.

Figure 3.14 illustrates the problem with slow fading by showing the performance of a Reed-Solomon (RS) coded OFDM spread spectrum system under Rayleigh fading with various Doppler frequencies. The signal has 64 carriers, a sampling frequency of 1 MHz, uses a RS(63,32) coder and has a processing gain of 16. The coding rate is justified in a later section. The interleaver depth is equal to the size of the RS codeword, 378 bits. As a reference, theoretical curves for flat fading performance with no diversity (L=1) and two-fold diversity (L=2) are also provided. Without using a very long interleaver, the coded OFDM spread spectrum system can perform well in a fast fading channel but not in a slow fading channel.

The RA-OFDM system approaches the flat fading problem by using coding and interleaving for fast fading channels and rate adaptation to track channel variation in slow fading. In other words, in a fast fading channel, the rate will be adjusted to the *average* channel conditions and coding and interleaving will be used to break up the fades while, in a slow fading channel, the rate adaptation will follow the fluctuations the channel. The coding and interleaving will remain when tracking the fading, it will just not be depended upon to mitigate the fading. In the following, we will use the finite-state Markov model for the Rayleigh fading to analyze the performance of the RA-OFDM scheme and compare this performance to that for a fixed rate system, i.e. a system which does not have variable processing gain.

The received signal SNR is partitioned into a finite number of intervals corresponding to the total number of states. The thresholds are ordered as $0 < \gamma_1 < \gamma_2 < \cdots < \gamma_M < \infty$ and these thresholds are chosen such that, taking into account the processing gain for each particular state, a desired BER of 10^{-4} is obtained at these thresholds. As a result, the BER is always less than or equal to 10^{-4} for all the channel states except S_1. Since fading in state S_1 can be arbitrarily deep, an infinite processing gain would be needed to guarantee that the BER $\leq 10^{-4}$. In the following, the adaptive

system adopts 2-state, 3-state and a 4-state adaptation models. The average normalized throughput $\overline{W}$ with the adaptive transmission scheme is given by

$$\overline{W} = \sum_{i=1}^{M} W_i \pi_i \tag{3.26}$$

where M is the number of adaptation levels, i.e. the number of states and π_i is the probability that the channel is in state i. W_i is the conditional normalized throughput given the state is i, defined as the average number of successfully transmitted information bits per unit time per unit bandwidth. This quantity is given by

$$W_i = \frac{(1 - P_{E|i})R_{c|i}}{P_{g|i}}, \tag{3.27}$$

where $P_{E|i}$, $R_{c|i}$ and $P_{g|i}$ are the packet error probability, coding rate and processing gain respectively, given channel is in state i. Figure 3.15 shows the throughput of the RA-OFDM system as compared to a fixed rate system. In this case, $R_{c|i}$ is set to 1 for all i, meaning that all the redundancy is from spreading only. It is clear from the figure that partitioning the channel SNR into finite number of discrete states and matching the processing gain of the RA-OFDM system to each of these states yields a huge improvement in the system throughput. One reason for this improvement is that the fixed rate system must be designed to provide the desired BER performance in the worst-case channel conditions, meaning that it must incorporate a large processing gain. Also, note that the performance of the adaptive rate system gets better when the number of states increases. This improvement is due to the fact that a closer match between processing gain and the channel conditions is achievable.

The above model assumes there are no state transitions during a packet duration. The following extends this model to allow at most one state transition during a packet duration under the assumption that the channel is

slowly varying. For example, if the packet length is 256 bits, $f_dT = 10^{-4}$, and $\pi_1 = \pi_2 = 1/2$, then the probability of two or more transitions occurring in a packet duration is 0.0014, which can be ignored. The conditional normalized throughput W_i is now given by

$$\begin{aligned} W_i = {} & W_{i|\text{no state transition}} * Prob(\text{no state transition}) + \\ & W_{i|\text{one state transition}} * Prob(\text{one state transition}) \end{aligned} \tag{3.28}$$

A 2-state adaptation is used for illustration as in Figure 3.16. Transmission rate in state S_2 is twice of that in state S_1. This factor has been considered when calculating the transitional probabilities at each state. Throughput contribution when there is no state transition is higher than the one when there is one state transition. With the increase of Doppler frequency and/or the number of states, the chance of state transition also increases. As a result, the total throughput decreases. This degradation gets worse with larger Doppler.

3.6 Discussion

The results that were presented show that, by adjusting the processing gain, it is possible to maintain an acceptable BER over a wide range of channel conditions. In the case of slow flat fading, being able to track channel variations provides a large gain in throughput since the link does not have to be designed for worst-case conditions. Additionally, it is advantageous to use FEC coding along with the processing gain. Analysis of the optimized trade-off between FEC coding and spreading will be performed in Chapter 4.

The proposed RA-OFDM uses a variable processing gain to deliver the best achievable data rate on a packet by packet basis over AWGN and multipath fading channels. The system uses FEC to supplement the processing

gain, frequency domain interleaving to exploit any available frequency diversity, and time domain interleaving to decorrelate any time domain variations which are too rapid to handle through processing gain variation. The overall adaptation strategy is to track variations in the channel whenever possible within the constraints of the access method and the packet length. The best approach is to adjust processing gain on a packet-by-packet basis, but this may not be feasible in some cases. The depth of the time domain interleaving would be determined by the limitations in the system's ability to track channel variations since the main purpose of the interleaving is to "break up" any fades that cannot be tracked. The ability to handle the slow fading case through processing gain adaptation mitigates the need for large interleaver depths, increases the overall throughput of the system and reduces the possibility of a complete loss of signal.

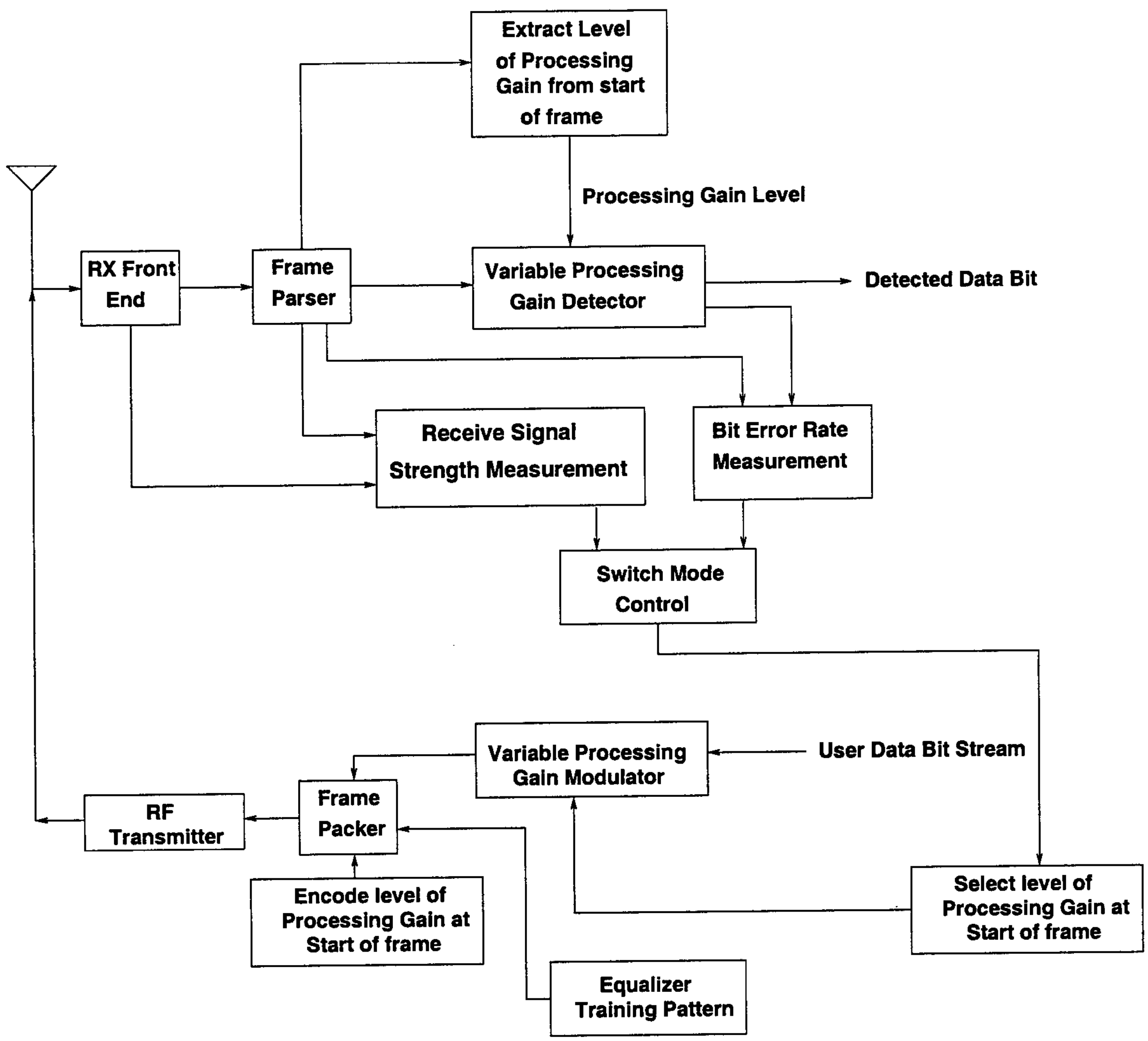

Figure 3.7: Block diagram for RSSI and BER switching system

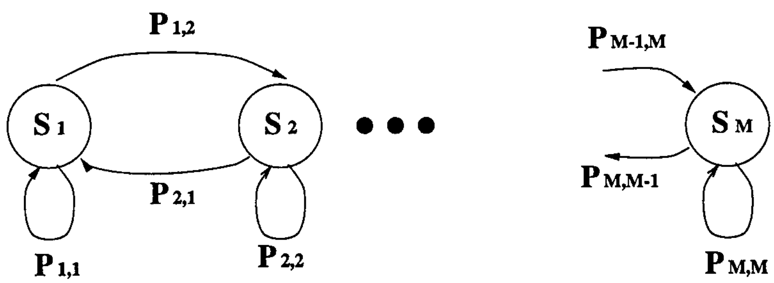

Figure 3.8: M-state Markov chain modeling a Rayleigh fading channel

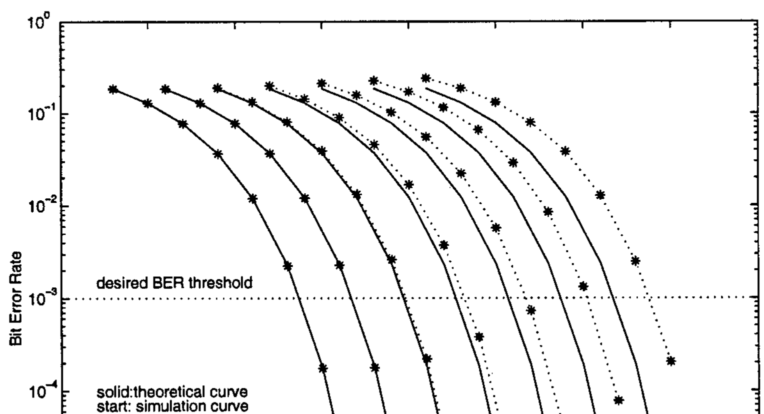

Figure 3.9: Rate adaptation with cyclical prefix

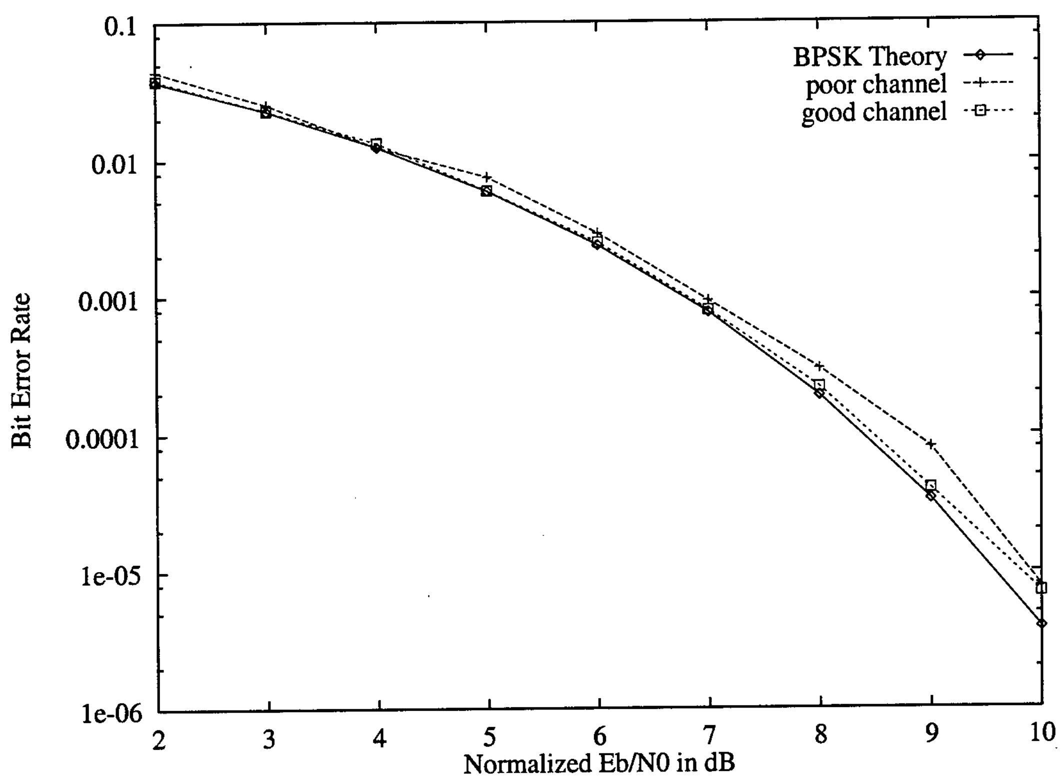

Figure 3.10: Equalizer performance with realistic packet structure

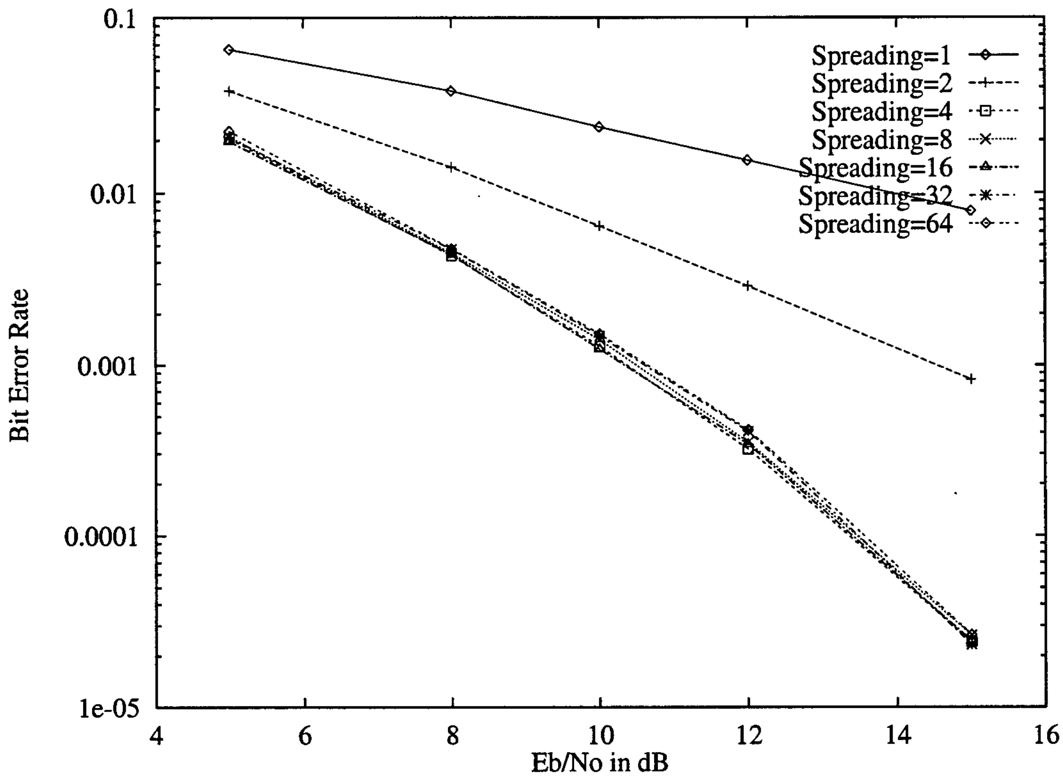

Figure 3.11: BER performance for a 4-ray selective fading channel, f_D=50Hz

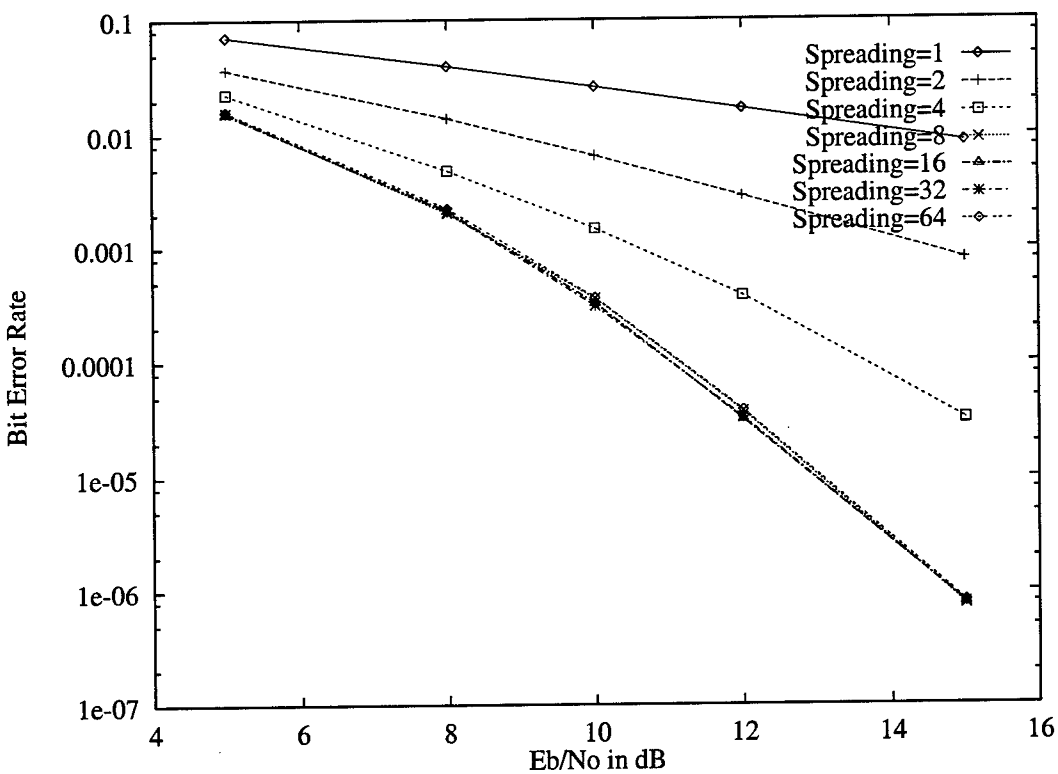

Figure 3.12: BER performance for a 8-ray selective fading channel, f_D=50Hz

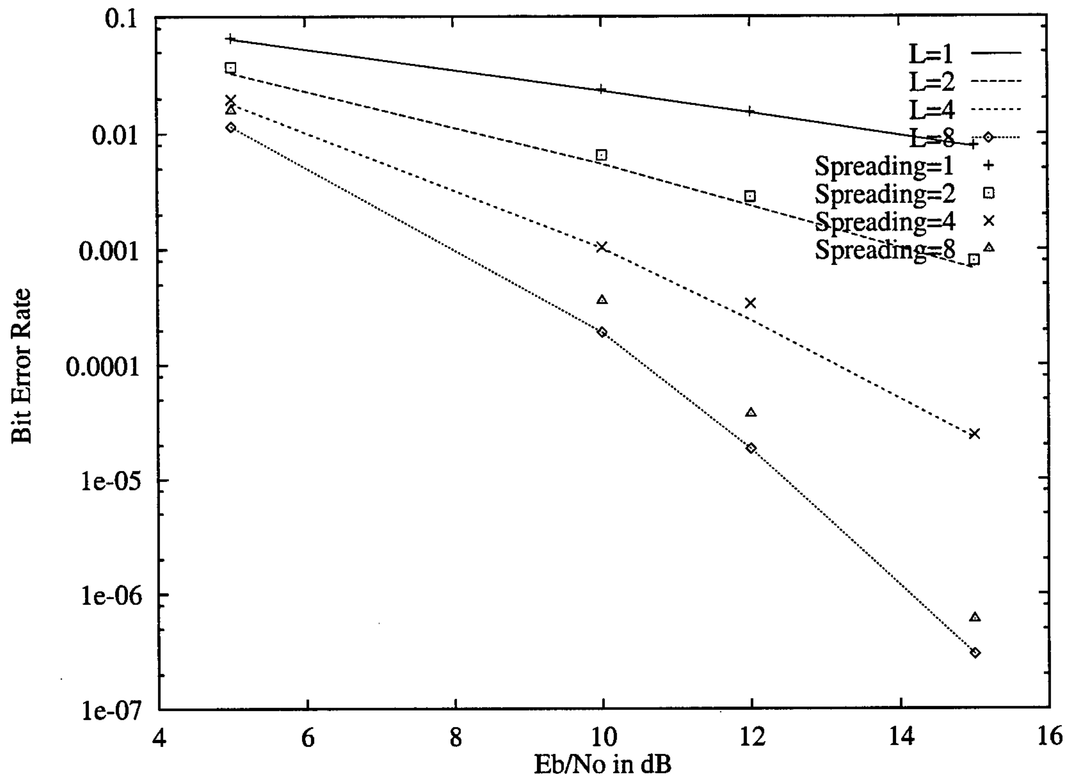

Figure 3.13: Maximum achievable diversity from various channel models

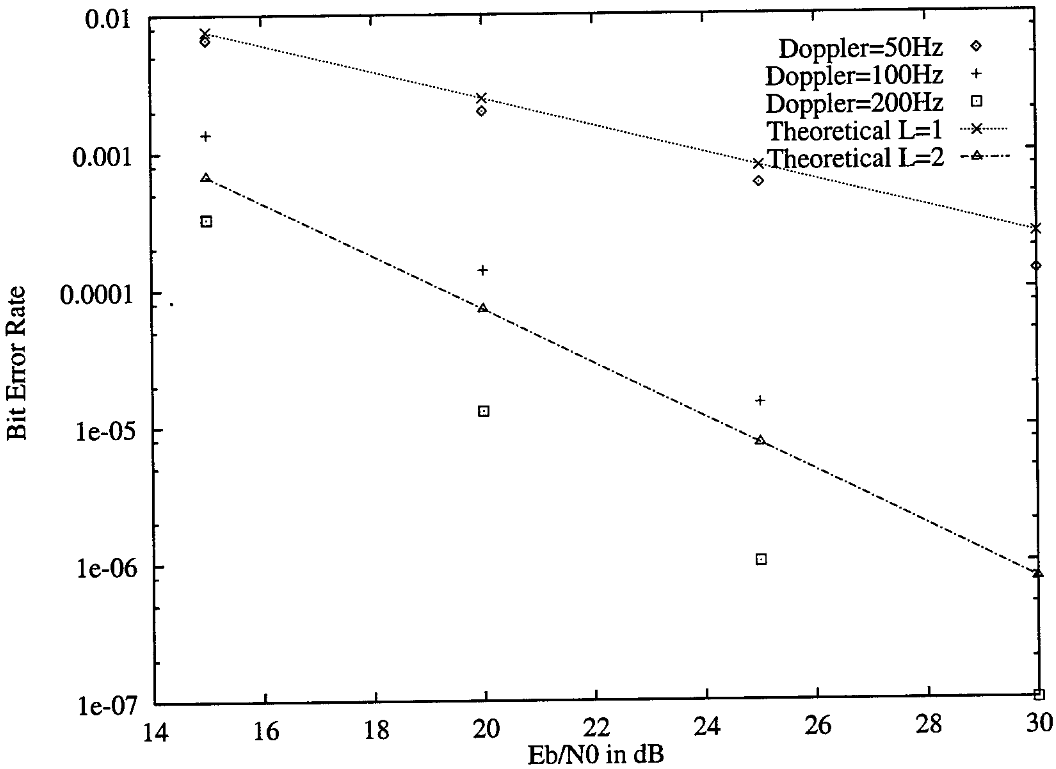

Figure 3.14: Reed-Solomon coded OFDM spread spectrum system in Rayleigh fading, FFT block size=64, (n,k)=(63,32), Pg=16

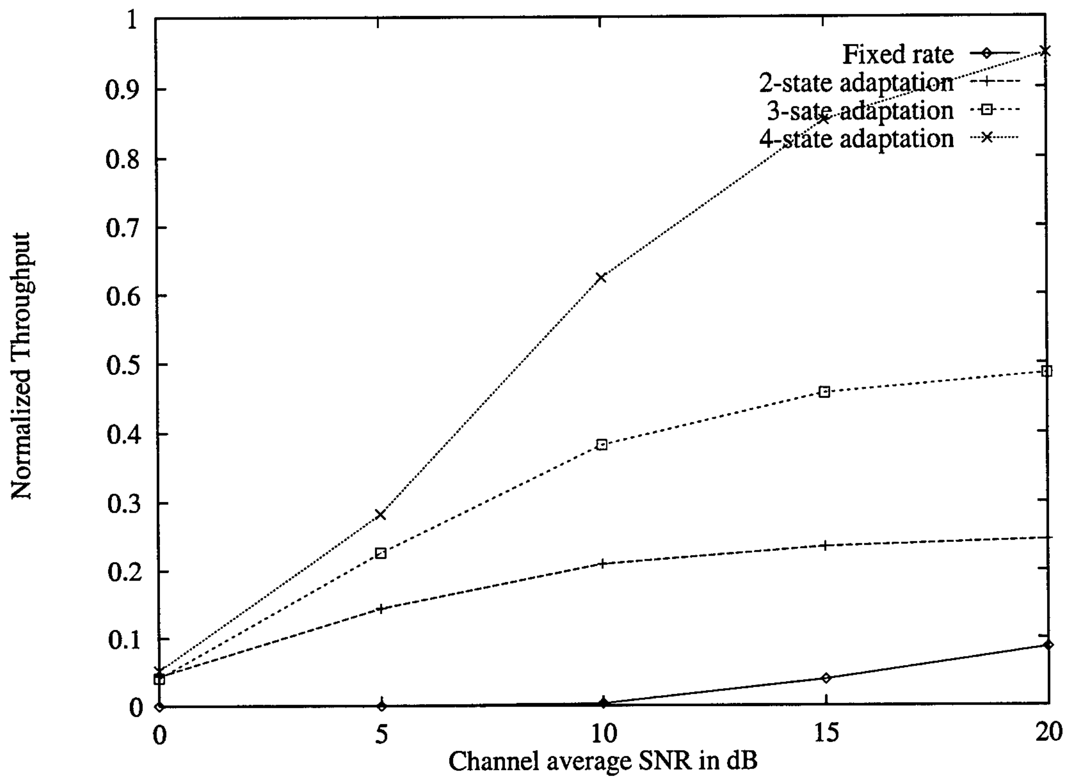

Figure 3.15: Maximum normalized throughput with fixed rate and RA-OFDM transmission schemes

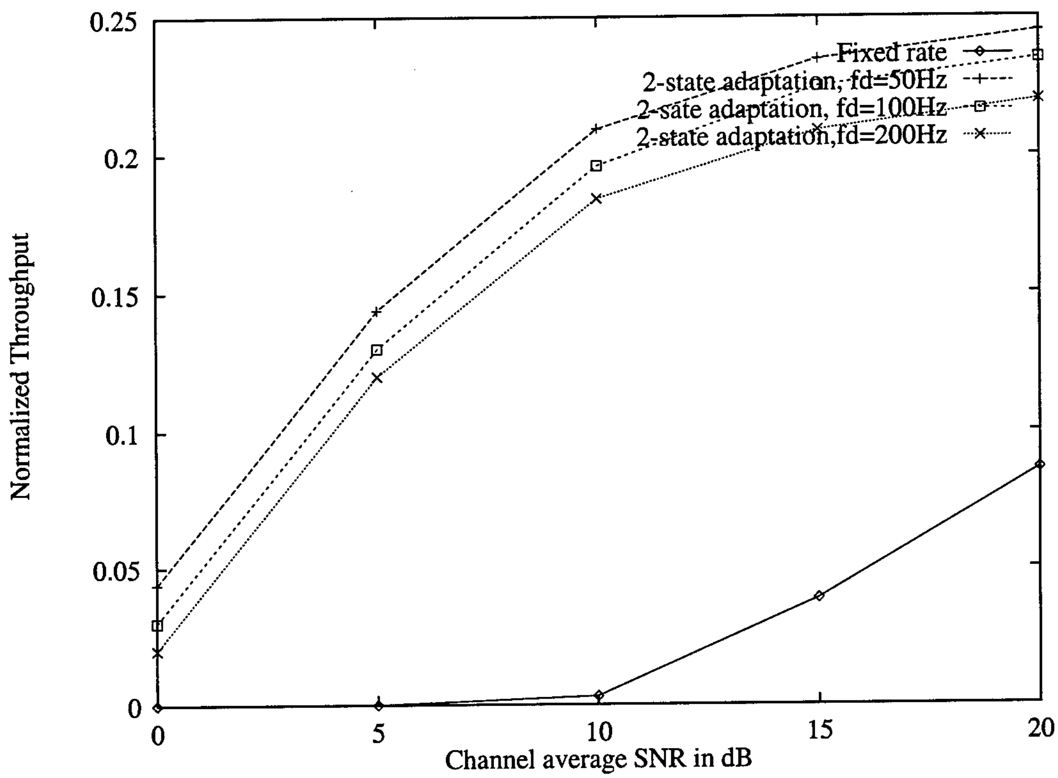

Figure 3.16: Maximum normalized throughput with fixed rate and RA-OFDM transmission schemes at different Doppler rate

Chapter 4

Adaptive Signaling with Packet Radio Network

4.1 Introduction

In the last chapter, the focus was on the physical layer issues of the RA-OFDM system. The emphasis of this chapter is to extend the analysis into the data link layer of a packet radio network to demonstrate the effectiveness of this rate adaptive signaling scheme.

The RA-OFDM system varies the processing gain and/or the modulation constellation size according to the changing channel conditions, such as the received signal-to-noise power ratio. This adaptivity results in users gaining access to the channel at different bit rates depending on their local channel conditions. The performance of a PRN using this signaling format is the major focus of this chapter. We study the network throughput problem under various access schemes. The advantage of adaptive system is first illustrated in a downlink (base-to-mobile) using time division multiplexing (TDM) scheme. It takes the best advantage of the adaptive system in terms of throughput. In addition to the importance of this scheme in downlink

channels, the maximum throughput derived from TDM can serve as a *ceiling benchmark* for the proposed adaptive PRN with other access techniques. The focus is then shifted to ALOHA and CSMA as these still are popular and cost effective ways to handle uplink data traffic.

Classic pure ALOHA [56, 57, 58, 59] and CSMA system analyses [60, 61] assume fixed length packets and Poisson arrival rates. In our adaptive system, due to the variable processing gain and/or constellation sizes, the mobile users transmit using variable packet durations with the number of data bits per packet held constant. For example, in an Additive White Gaussian Noise (AWGN) channel, the mobiles near the base station will have high SNR and they can select a larger constellation size and/or lower processing gain to shorten the packet duration. With the increase in packet success rate due to fewer collisions, the overall system throughput is increased. On the other hand, mobiles at the fringe of the coverage area are usually in worse channel conditions and in order to combat the unfavorable conditions, data rate is traded off for quality. Mobiles can select smaller constellation size and/or larger processing gain. There are several papers [62, 63, 64, 65] studying networks with variable packet lengths. However, none of these are applicable to the adaptive system analysis because all of these studies assume constant user data rate and packet lengths are independent of channel conditions. The author introduces a method to analyze network throughput using *variable packet lengths due to variable user data rate.* In addition, we incorporate the packet error rate due to the AWGN into our analysis as in [66].

Given the built-in physical layer adaptivity of our proposed system, various network system parameters can be optimized. These can include network throughput, total transmit power, traffic delay, network buffer memory, traffic priority. For instance, in battery operated or Low Probability of Interception (LPI) driven applications, the goal could be to minimize transmit power while subject to the BER constraint. For delay sensitive traffic, the

goal could be to maximize the throughput subject to delay constraint. For variable priority traffic, the goal could be to ensure higher priority traffic to get through with minimum BER. In this report, we focus only on network throughput optimization subject to the desired BER constraint.

4.2 RA-OFDM System for Packet Radio Networks

This report is premised on the use of a physical layer that can adapt to the channel quality in a way that maximizes the data rate while maintaining a BER that is below a maximum acceptable level.

The proposed system selects the modulation parameters, specifically, the processing gain, on a packet-by-packet basis according to the channel conditions in order to achieve the maximum data rate while maintaining a desired bit error rate. Figure 4.1 shows an example of the processing gain selection procedure. In this example, BPSK and OFDM-SS modulation is used. Seven different processing gains from 1 to 64 (doubling each step), corresponding to seven user data rates, can be selected for a mobile user at any given time. At a given SNR, a larger processing gain corresponds to a lower data rate and a better BER performance. More importantly, a desired BER can be maintained over a wide range of SNR values, e.g. a bit error rate of 10^{-3} can be maintained over the range of -12 to +12 dB, by the appropriate control of the processing gain (and data rate).

In this report we will be comparing the throughput performance of a fixed rate system with an adaptive system. Refer to Chapter 3 for the packet structure details.

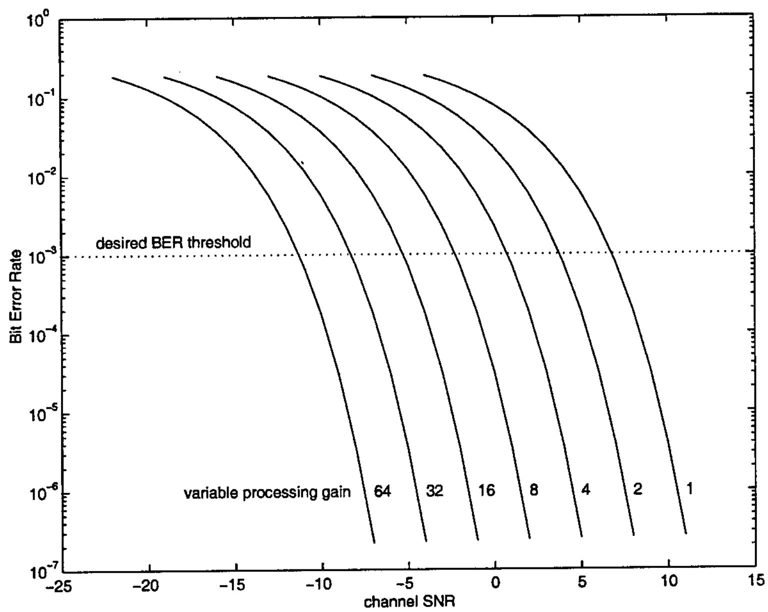

Figure 4.1: Processing gain selection procedure

4.3 Throughput Analysis of the Adaptive Packet Radio Networks

We have proposed an adaptive transmission scheme which transmits at a higher information rate (i.e. lower processing gain) when the received SNR is high, and a lower information rate (i.e. higher processing gain) when the received SNR is low. With the underlying adaptive engine, we want to study the networking aspects of the system.

4.3.1 Network Throughput Analysis, Downlink (base-to-mobile) using TDM

The adaptive system achieves maximum throughput using a fixed access scheme. A typical example involves the downlink capacity calculation using time division multiplexing. We start the analysis by introducing an analytic framework. This same framework is shared later for other contention-based access schemes.

The network under study consists of a base station with mobile users in a circular surrounding peripheral with radius R. Assume users are uniformly distributed (in users/unit area) in the cell site. Therefore the probability density function (pdf) of the user density is uniform in θ and varies in the distance from the center, r, as,

$$f(x,y) = \frac{1}{\pi R^2}, \quad f(r,\theta) = \frac{1}{\pi R^2} r, \quad f(r) = \int_0^{2\pi} f(r,\theta) d\theta = \frac{2}{R^2} r.$$

Initially assume a free-space model where attenuation is proportional to r^2 [67] and assume that the processing gain is adjusted with respect to the distance between the base station and mobile to maintain a constant BER. To achieve this, divide the circular cell into seven rings, indexed from 1 at the

center to 7 at the edge. Assume for example that the maximum allowable BER is 10^{-6}, meaning that the fixed signaling format must provide BER $= 10^{-6}$ at the outer region and, consequently, will provide much lower values for the inner rings. Conversely, the adaptive rate system strives to maintain a fixed BER of 10^{-6} by using larger constellation size and/or less processing gain for the inner rings, resulting in shorter packet durations. For easier interface with the OFDM implementation, processing gain starts with 1 in the most inner ring and doubles for each subsequent ring. In other words, if i is the ring index from 1 to 7, then processing gain for each ring is 2^{i-1}. Based on the second order path loss model, in order to maintain a constant received signal-to-noise ratio (*after despreading*) at each ring boundary, the radius of ring i is $R_i = R_1(\sqrt{2})^{i-1}$, while $R_7 = R$ which is the cell boundary. Given the above user population pdf function $f(r)$, the probability that a user is in ring i is thus $\int_{R_{i-1}}^{R_i} f(r)dr$. We will use this method again for other user population profiles in the later section.

Tables 4.1 and 4.2 show parameters for the adaptive and fixed rate systems, in which R_i, Pg_i, r_i, T_i, $Tput_i$, Pb_i and BER_i are the ring index, processing gain, ring boundary, packet duration, individual throughput, probability user inside ring and bit error rate respectively.

Notice that the BER at each ring of the adaptive system is constant. This is the result of variable processing gain. The BER is calculated at the outer edge of each ring boundary meaning that the BER is generally somewhat better than 10^{-6} and, therefore, the corresponding throughput analysis produces a lower bound on performance. For the fixed rate system, constant packet duration T and constant processing gain are used in all seven rings. Therefore the BER in each ring decreases to virtually zero as a user approaches the base station.

Table 4.1: Adaptive system parameters for seven-ring structure

R_i	Pg_i	r_i	T_i	$Tput_i$	Pb_i	BER_i
1	1	R/8	T/64	64	1/64	10^{-6}
2	2	$\frac{\sqrt{2}}{8}R$	T/32	32	1/64	10^{-6}
3	4	R/4	T/16	16	1/32	10^{-6}
4	8	$\frac{\sqrt{2}}{4}R$	T/8	8	1/16	10^{-6}
5	16	R/2	T/4	4	1/8	10^{-6}
6	32	$\frac{\sqrt{2}}{2}R$	T/2	2	1/4	10^{-6}
7	64	R	T	1	1/2	10^{-6}

Table 4.2: Fixed rate system parameters for seven-ring structure

R_i	Pg_i	r_i	T_i	$Tput_i$	Pb_i	BER_i
1	64	R/8	T	1	1/64	0
2	64	$\frac{\sqrt{2}}{8}R$	T	1	1/64	0
3	64	R/4	T	1	1/32	$6.3 * 10^{-81}$
4	64	$\frac{\sqrt{2}}{4}R$	T	1	1/16	$1.6 * 10^{-41}$
5	64	R/2	T	1	1/8	$9.7 * 10^{-22}$
6	64	$\frac{\sqrt{2}}{2}R$	T	1	1/4	$9.8 * 10^{-12}$
7	64	R	T	1	1/2	10^{-6}

Now consider a contention-free access scheme such as a TDM BS to MS link and compare the throughput for the fixed and adaptive systems. Assume that the transmission rate for both systems is C bits/sec at the fringe area and very low BER is maintained so that we can neglect the packet errors due to AWGN. Denote S_i as the individual throughput from each ring, then the

maximum throughput in bits/sec for the fixed rate system is,

$$\begin{aligned} S_{fixed} &= \sum_{i=1}^{7} S_i * Prob(\text{user in ring i}) * C \\ &= (1/64 + 1/64 + 1/32 + 1/16 + 1/8 + 1/4 + 1/2) * C \\ &= C \text{ (bits/sec)} \end{aligned}$$

For the adaptive counterpart,

$$\begin{aligned} S_{adaptive} &= \sum_{i=1}^{7} S_i * Prob(\text{user in ring i}) * C \\ &= (64/64 + 32/64 + 16/32 + 8/16 + 4/8 + 2/4 + 1/2) * C \\ &= 4C \text{ (bits/sec)} \end{aligned}$$

If we normalize the throughput with respect to the transmission rate of the fixed system, the throughput of the fixed and adaptive system are 1 and 4 respectively, i.e. we get a potential four-fold increase in throughput using our adaptive system.

Having users uniformly distributed over a circular region is not representative of many potential applications of a PRN. In a commercial application like an indoor office environment, users tend to be clustered rather than uniformly distributed in two dimensions. One realistic population distribution is along a building corridor. In such case, the previous assumption that user population density linearly increases with distance from the hub is replaced by a flat, uniform density. In other words, the user pdf has changed from $f(r) = \frac{2}{R^2}r$ into $f(r) = \frac{1}{R}$. The same distribution can be found in an outdoor application such as coverage area along a highway. Figure 4.2 illustrates the two user population profiles for a case of $R = 100$.

For the flat uniform density, the maximum throughput of the adaptive

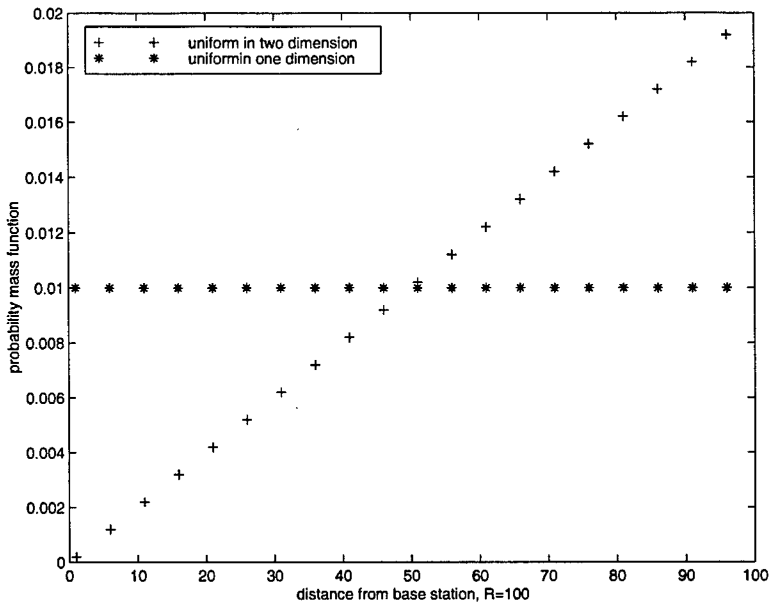

Figure 4.2: Linear versus flat user population profiles

system is

$$
\begin{aligned}
S_{adaptive} &= \sum_{i=1}^{7} S_i * Prob(\text{user in ring i}) * C \\
&= (64 * (1/8) + 32 * (\sqrt{2}/8 - 1/8) + 16 * (1/4 - \sqrt{2}/8) \\
&\quad +8 * (\sqrt{2}/4 - 1/4) + 4 * (1/2 - \sqrt{2}/4) + 2 * (\sqrt{2}/2 - 1/2) \\
&\quad +1 * (1 - \sqrt{2}/2)) * C \\
&= 12.9C \text{ (bits/sec)}
\end{aligned}
$$

This result represents an almost thirteen-fold increase in system throughput. Note that the throughput of the fixed rate system is not dependent on user pdf, hence is again equal to C here.

Although there are some simplifications in the analysis for the downlink capacity using TDM, it serves to illustrate the potential increase in capacity

offered by the adaptive scheme. Such a scenario is by no means unpractical, since in applications such as wireless Internet services downlink capacity is usually of great importance.

Next we will extend the same framework into uplink throughput analysis. For data dominant traffic, random access schemes such as ALOHA and CSMA are still the popular and cost effective access techniques and they are the focus of the following sections.

4.3.2 Network Throughput Analysis for Pure-ALOHA Adaptive PRN

In a pure-ALOHA system, mobile users randomly send their packets to the central base station and wait for the return of a positive acknowledgement upon the detection of an error-free packet. A user retransmits its packet if an acknowledgement has not been received within a given period of time. Our analysis uses the widely employed approximation of an infinite population of users generating packets according to a Poisson process with parameter λ, e.g. [60, 61, 62, 63, 64, 65, 68, 69]. For the fixed rate system, all packet transmissions are of the same duration T. For the adaptive system, the actual information bit rate changes with the channel conditions. This equivalently translates into variable packet duration which depends on the channel conditions. When observing the channel, packets (new and retransmitted) arrive according to a Poisson process with parameter g packets/sec.

The channel throughput, S, is defined as the average number of packets successfully transmitted in an interval of the packet duration. The parameter $G = gT$ is defined as the *normalized offered load.* Roberts [66] extended the classic throughput analysis to include the effects of an AWGN channel,

$$S = Ge^{-2G}(1 - P_{pe})(1 - P_{ae}) \tag{4.1}$$

in which P_{pe} is the probability that a packet is not accepted due to channel noise errors and P_{ae} is the probability of acknowledgement error. If we further simplify the channel to assume an error-free acknowledgement path, the throughput is expressed as,

$$S = Ge^{-2G}(1 - P_{pe}). \tag{4.2}$$

For our adaptive system, the throughput will be different in each ring. We now calculate the expected throughput for a user in ring i. Denote the transmission duration of the current user at ring i as t_i, and the period for a collision user at ring j as t_j. They are independent random variables. The vulnerable window size is $t_i + t_j$. Denote S_i as the system throughput conditioned on current user active in ring i and P_i, P_j as the probability that the users are in ring i and j, respectively. Now,

$$\begin{aligned} S_i &= gTProb(\text{no collision})\left(1 - P_{\text{bit error at ring i}}\right)^N \\ Prob(\text{no collision}) &= \prod_{j=1}^{7} Prob(\text{no collision with user in ring j}) \\ &= \prod_{j=1}^{7} e^{-P_j g(t_i+t_j)} = e^{-g\left(t_i+\sum_{j=1}^{7} P_j t_j\right)}. \end{aligned}$$

Keep in mind that independent of the data rate of the user, the successful packet transmitted is N bits long. And since P_b is the probability of bit error *after despreading*, the packet length in calculating packet error due to AWGN is also N bits long.

Therefore, the total system throughput is

$$S_{adaptive} = \sum_{i=1}^{7} S_i P_i. \tag{4.3}$$

The fixed rate system is a special case in which $t_i = T$ for all i. If we plug this into the above analysis, the fixed rate system throughput conditioned

on current user active in ring i is

$$\begin{aligned} S_{\text{i fixed}} &= gTe^{-2gT}\left(1 - P_{\text{bit error rate at ring i}}\right)^N \\ &= Ge^{-2G}\left(1 - P_{\text{bit error rate at ring i}}\right)^N \end{aligned} \tag{4.4}$$

Therefore, the total system throughput is

$$S_{fixedrate} = \sum_{i=1}^{7} S_{\text{i fixed}} P_i, \tag{4.5}$$

the same result as the classic ALOHA analysis.

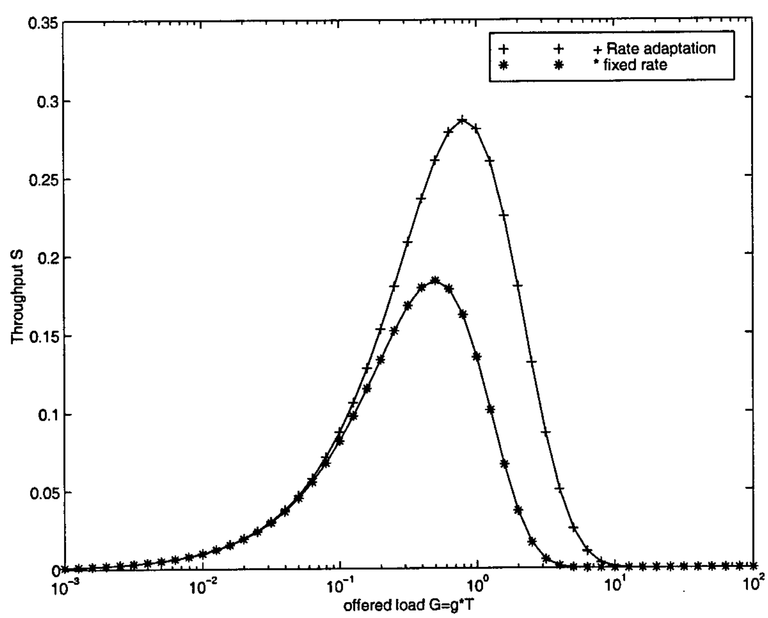

Figure 4.3: Throughput analysis, ALOHA system, moderate channel error, $P_b = 10^{-6}$ at ring 7

Figures 4.3, 4.4 and 4.5 show the adaptive and fixed ALOHA system throughput for different channel error rates. The packet length, N, is chosen

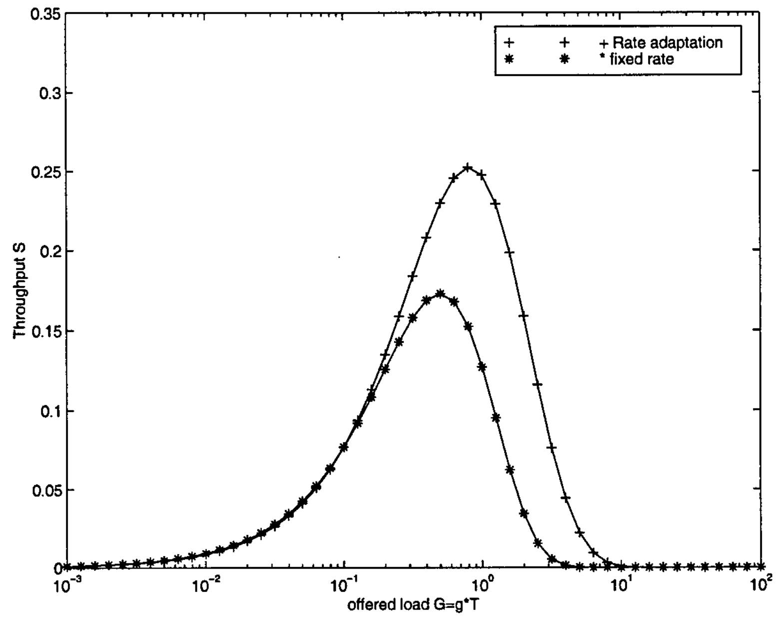

Figure 4.4: Throughput analysis, ALOHA system, high channel error, $P_b = 10^{-3}$ at ring 7, N=128

to be 1280 bits unless otherwise specified. Across all the loading conditions, we see a consistent throughput performance improvement for the adaptive ALOHA system. Note that when the BER is 10^{-3}, N is reduced to 128 to reduce the packet loss due to AWGN.

4.3.3 Pure-ALOHA, Different Path Loss Models and User Population Profile

According to [67], both theoretical and measurement-based propagation models indicate that the received signal power is proportional to $\left(\frac{r_0}{r}\right)^n$, where n is the path loss exponent which indicates the rate at which the path loss

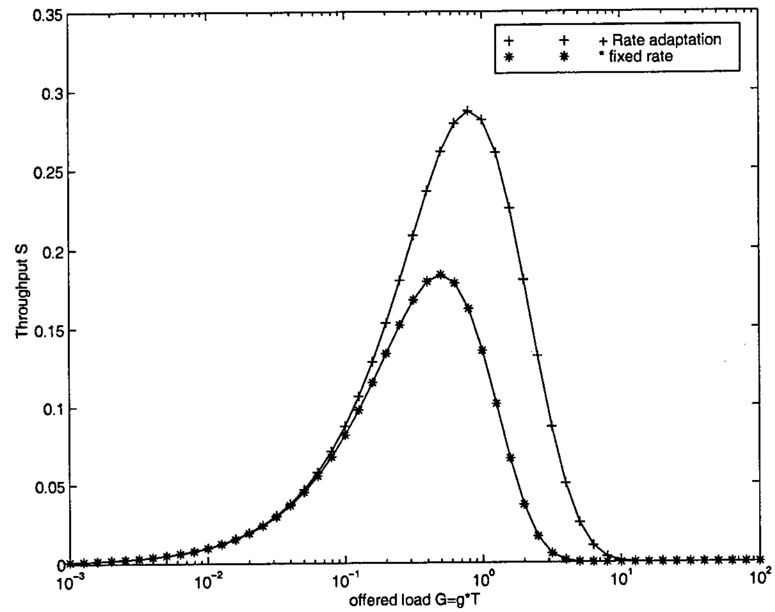

Figure 4.5: Throughput analysis, ALOHA system, almost error free channel, $P_b = 10^{-12}$ at ring 7

increases with distance, r_0 is the reference distance which is determined from a measurement close to the transmitter, and r is the separation distance between base and mobile. For the above results, free space propagation ($n = 2$) was assumed. For a mobile radio channel, n is usually between 3 and 4 [70]. A larger value of n will increase the performance gain provided by the adaptive system since the greater attenuation results in a larger data rate disparity between the fixed and adaptive system at the inner rings. Figure 4.6 shows the improvement associated with various values of n.

Next we want to analyze system throughput under flat uniform user distribution. Such user profile is typical in an indoor office environment or an outdoor highway situation. This distribution provides even more room for

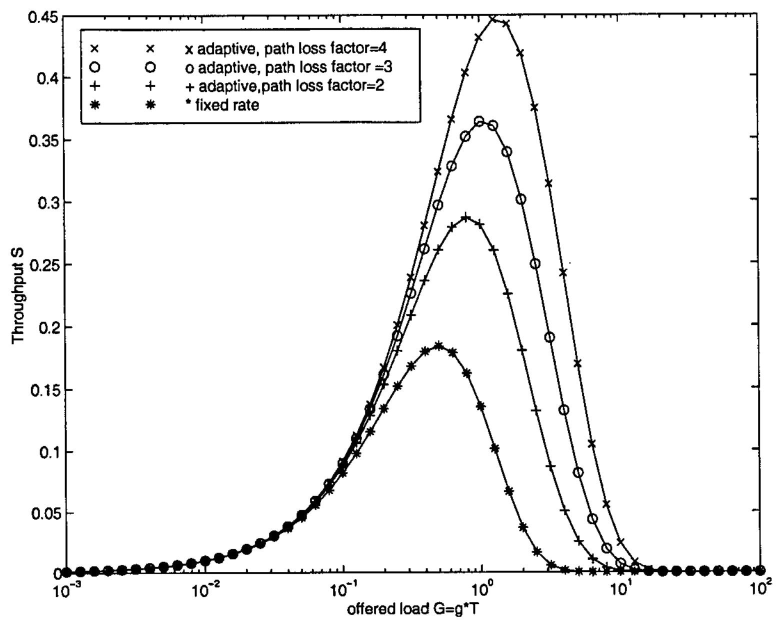

Figure 4.6: ALOHA system throughput with various path loss factors

throughput improvement with rate adaptation because the reshaping of the pdf puts more users closer to the base station where the rate can be boosted up. Figure 4.7 shows this improvement trend. Keep in mind that the fixed rate system throughput does not depend on user population profile.

Figure 4.8 shows where the added capacity comes from by breaking down the throughput contribution with respect to ring index for both the flat and linear user profiles. It is obvious from the breakdown that the majority of the throughput improvement comes from the inner rings where packet lengths are much shorter resulting a much higher chance of getting through the network without collision. The throughput at each ring of the linear profile increases exponentially because of the population increases in the same way. Therefore,

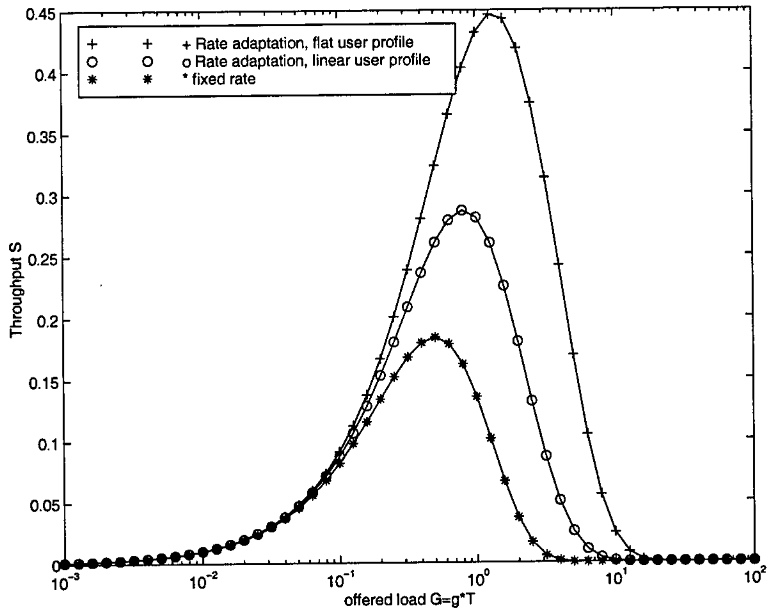

Figure 4.7: ALOHA system throughput with various user population profile

not only does the uniform profile deliver a higher total throughput, it tends to offer better fairness to users at each ring.

With the fixed rate system, once a user goes outside the fringe boundary, the BER can become so high that a link can not be established or maintained. This type of "hard boundary" is not acceptable for military applications and can be undesirable in commercial applications. The adaptive system can maintain connectivity for users outside the main coverage area by allowing these users to use an even larger processing gain. If the adaptive system still operates with the number of data bits per packet held constant, then the packet duration increases, as users get further away from the base station. As a result, supporting users outside the main coverage area could require

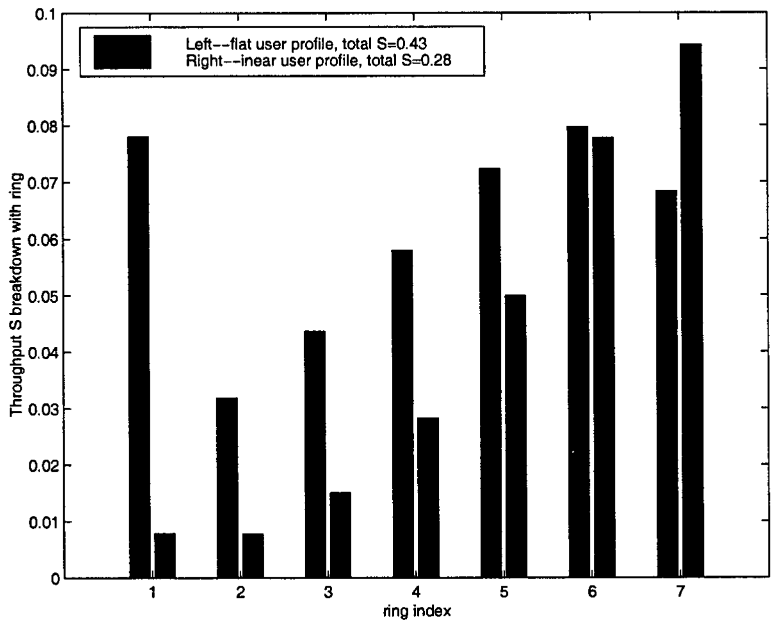

Figure 4.8: ALOHA system throughput breakdown with ring index, flat vs. linear user profile

even larger packet durations which can potentially become a major bottleneck to the system throughput. A long duration not only makes the long packet itself difficult to get through, but also increases the chance of collision with other shorter packets. One alternative is to reduce the bit rate of the outside users by forcing fewer number of bits per packet for them. Another one is to use a contention-free access scheme. There exists here, a balance between continuing critical service for outside users and maintaining decent throughput for inner users. The adaptive system is more flexible to maintain this balance.

4.3.4 Network Throughput Analysis for Nonpersistent CSMA Adaptive PRN

We now extend our network throughput analysis to nonpersistent CSMA. We adopt a model similar to the one used in the ALOHA system and extend the analysis in [61] to our adaptive system. Denote by $\tau/2$ the propagation delay from the edge of the cell to base station and define $a = \tau/T$ to be the normalized propagation time. T is the transmission duration of a packet for the fixed rate system. Thus, for a user at ring i (with radius R_i), delay of $\tau_i = \frac{\tau}{2} + \frac{\tau}{2}R_i/R$ will occur before all users hear its transmission.

We denote by $\tilde{B}$ the duration of the busy transmission period, and by B its mean. Let $\tilde{U}$ be the time duration within the transmission period in which a successful packet is being transmitted, with mean U. Let $\tilde{I}$ be the duration of the idle period with mean I. The cycle length is clearly $\tilde{B} + \tilde{I}$ and the throughput is given by

$$S = \frac{UR_{effective}}{B+I},$$

where $R_{effective}$ is the effective data rate which is inversely proportional to the processing gain and it accounts for the higher data rates for the inner rings.

The idle period duration is the same as the duration between the end of packet transmission and the arrival of the next packet. Because the packet scheduling is memoryless, $\tilde{I}$ is exponentially distributed with mean

$$I_{adaptive} = \frac{1}{g}. \tag{4.6}$$

The expected useful time U_i, given that the current user is active in ring i, is given by

$$\tilde{U}_i = \begin{cases} t_i & \text{Successful period} \\ 0 & \text{Unsuccessful period} \end{cases} \tag{4.7}$$

If P_{suc} denotes the probability of successful transmission of a packet, and P_{b-i} is the BER at ring i, the conditional U_i is

$$\begin{aligned} U_i = E[\tilde{U}_i] &= t_i P_{suc} \left(1 - P_{b-i}\right)^N \\ &= t_i Prob(\text{no packet arrives in } [t, t+\tau_i]) \left(1 - P_{b-i}\right)^N \\ &= t_i e^{-g\tau_i} \left(1 - P_{b-i}\right)^N . \end{aligned} \tag{4.8}$$

To compute B_i, the average transmission duration at ring i, we want to consider it as a "sum" of collisions with different numbers of contending users, i.e. $0, 1, 2, \cdots n$ contending users. Given a user starts transmitting at time t, the vulnerable window is $[t, t+\tau_i]$. The number of arrivals during that window, including new and backlogged, follows the Poisson distribution, i.e.

$$Prob(n \text{ arrivals in vulnerable window}) = \frac{(g\tau_i)^n}{n!} e^{-g\tau_i}. \tag{4.9}$$

What is a practical range for propagation delay τ_i? In most of our analysis, the packet size is chosen to be medium to large ($N = 1280$) in order to fully utilize the adaptive advantage. Our system is targeted to high speed indoor commercial/medium speed outdoor tactical applications. For an indoor WLAN, we assume a minimum data rate of 1 Mbps. For a cell radius of about 10,000 ft, this translates to $a \simeq 0.01$. This value of a is also valid for an outdoor application where the data rate is on the order of hundreds of kbits/sec, so both the packet duration and propagation delay increase. Given $g\tau_i = a * gT \simeq 0.01G$, then for almost all the loading conditions of interest ($G < 10^2$), $g\tau_i$ is small, and equation (4.9) approaches zero quickly as n increases. Therefore we only consider lower order terms (n=0 and 1) for the majority of the loading conditions and a few higher order terms ($n \geq 2$) for very heavy loading conditions. We will focus on the lower order terms for the analysis now and verify that the approximation is very accurate later.

Denote B_i as the average transmission time given that user A starts transmitting in ring i at time t, and that users B, C etc. potentially contend with A. Then

$$\begin{aligned} B_i \;\leq\; & e^{-g\tau_i} * (t_A + \tau_i) + g\tau_i * e^{-g\tau_i} * (\overline{\max(t_A, t_B)} + 2\tau_i) \qquad (4.10) \\ & + \text{higher order terms...} \end{aligned}$$

The right side is a upper bound because, $t+\tilde{Y}$ denotes the time at which the longest interfering packet was scheduled within a transmission period that started at t and we are bounding $\tilde{Y}$ with τ_i. Since all the packet durations are larger than τ_i, the approximation is accurate. When there are two contending users, $\overline{\max(t_A, t_B)}$ in the second term of the equation, is the weighted average over seven rings for user B given that user A is in ring i. The same reasoning applies to the higher order terms.

Putting all these results together we can evaluate $S_i = U_i R_{effective}/(B_i + I)$ and the system throughput

$$S_{adaptive} = \sum_{i=1}^{7} S_i P_i. \qquad (4.11)$$

The fixed rate system is a special case in which all packets are of duration T, therefore

$$I_{fixed} = \frac{1}{g} \qquad (4.12)$$

$$U_{i,fixed} = E[\tilde{U}] \;=\; Te^{-g\tau_i}\left(1 - P_{b-i}\right)^N$$

and, since all $t_i = T$,

$$B_{i,fixed} \simeq [T + 2\tau_i]\,. \qquad (4.13)$$

Given I, U_i and B_i, the system throughput can be evaluated. Figure 4.9 compares the adaptive system performance with that for the fixed rate system.

As the figure shows, the approximation method using only the lower order terms is accurate, especially for low to medium loading conditions. We will continue to use this approximation unless otherwise specified. Figures 4.10 and 4.11 show the performance for various values of BER. Note that for BER $= 10^{-3}$, the packet length N is intentionally shortened to 128 and, and correspondingly, the value a becomes 0.1.

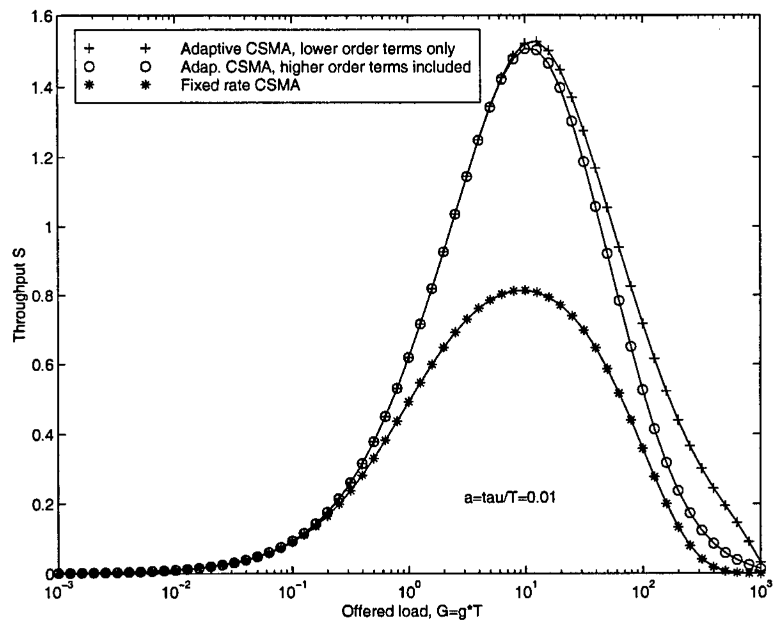

Figure 4.9: Throughput analysis, CSMA system, moderate channel error, $P_b = 10^{-6}$ at ring 7

For light loading, the throughput is almost equal to the offered load even for the fixed rate system, so there is little room for improvement from adaptive system. As the load increases into the moderate area, we can see a significant throughput increase from the adaptive approach, as the throughput is nearly doubled. Once the load becomes too high, we can see that both

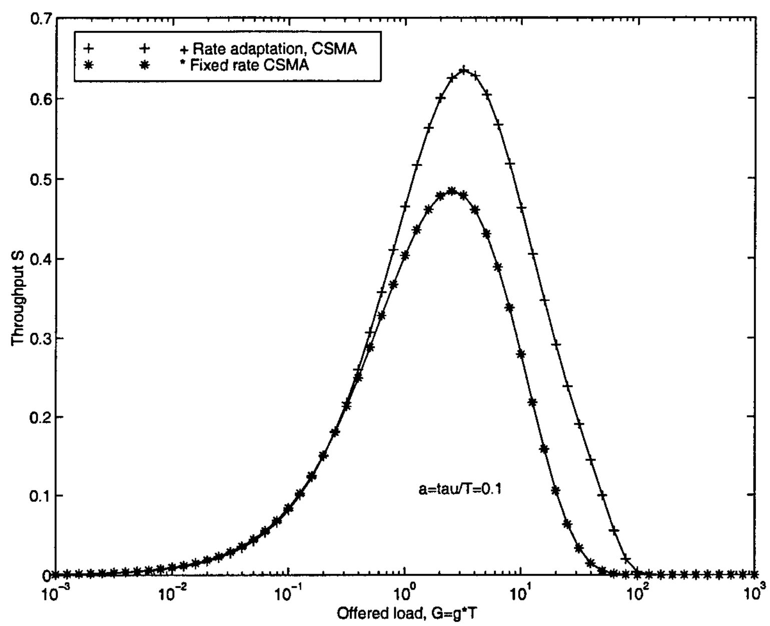

Figure 4.10: Throughput analysis, CSMA system, high channel error, $P_b = 10^{-3}$ at ring 7, N=128

systems suffer a large performance degradation. This is typical for random access schemes, however, the adaptive system degrades more slowly than the fixed one.

Figure 4.12 shows the performance of these systems for various user profiles. Under the one dimensional flat user profile, the adaptive system delivers about three times the throughput of its fixed rate counterpart. This increased throughput occurs because more users now stay in inner rings where data rate is much higher.

Paralleling the analysis of ALOHA, we plot the performance of the system under various path loss models in Figure 4.13. Again, for mobile radio channel, adaptive system can triple the system throughput compared to a

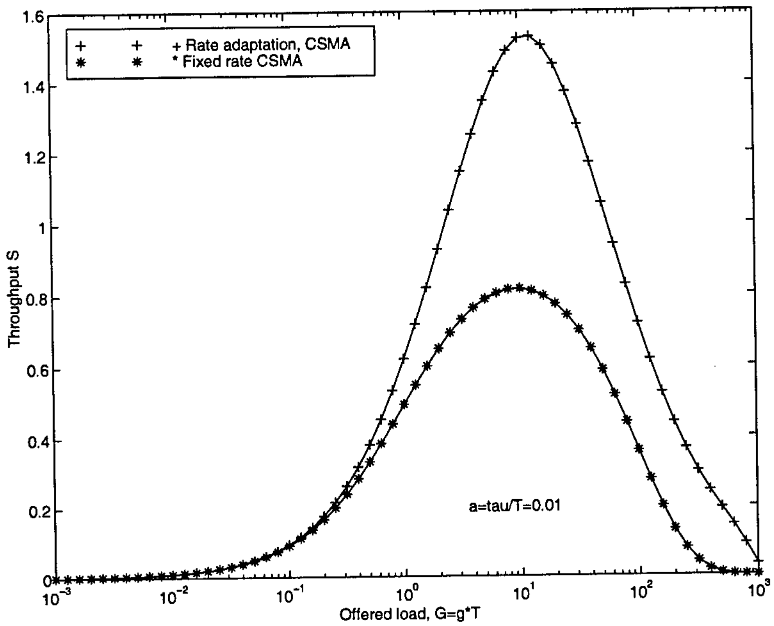

Figure 4.11: Throughput analysis, CSMA system, almost error free channel, $P_b = 10^{-12}$ at ring 7

fixed one.

Throughput versus normalized offered load, G, for various values of normalized propagation time a is studied. Figure 4.14 shows these results for a linear user profile while Figure 4.15 shows the results for a flat user profile. As is expected, the lower a becomes the better the performance. As a approaches 0, the system approaches a collision free situation. It is very interesting to compare the system throughput for both the fixed rate and adaptive system under such a circumstance. For the fixed rate system, based on the above analysis, throughput approaches 1 matching the classic NP-CSMA result of $G/(G+1)$. For the adaptive system, $a \to 0$ creates a scenario very similar to the downlink capacity using TDM which we dis-

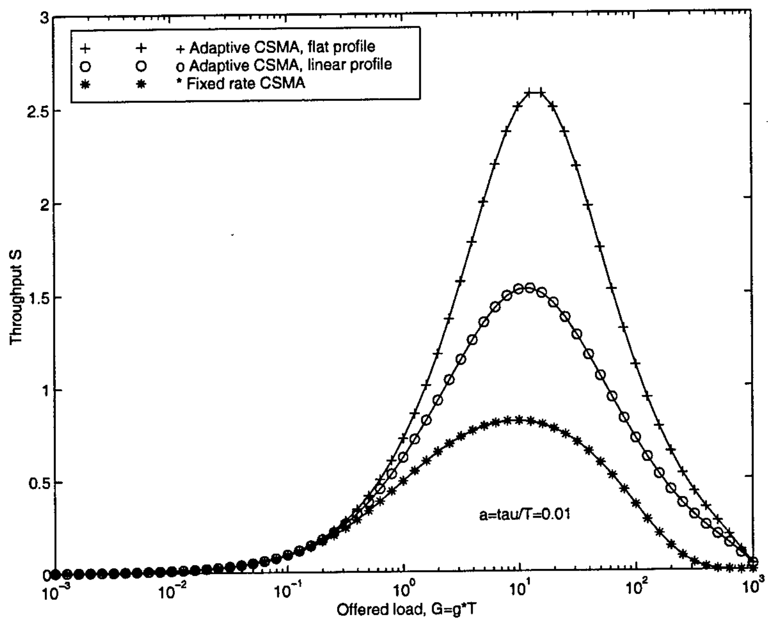

Figure 4.12: Throughput analysis, CSMA system, various user profile

cussed earlier. Throughput approaches 4 and 12.9, respectively, under linear and flat user profiles. These results match the maximum throughput results we derived for the TDM cases. These observations are important. Based on our earlier discussion of valid values for the normalized propagation delay a, 0.01 corresponds to a cell radius of about 10,000 ft (about 2 miles). For most indoor applications, cell sizes are much smaller, resulting in a much smaller value for a. The same discovery can be also utilized in an outdoor application to favor the pico-cells design in which a is intentionally kept very small to improve capacity in high traffic areas.

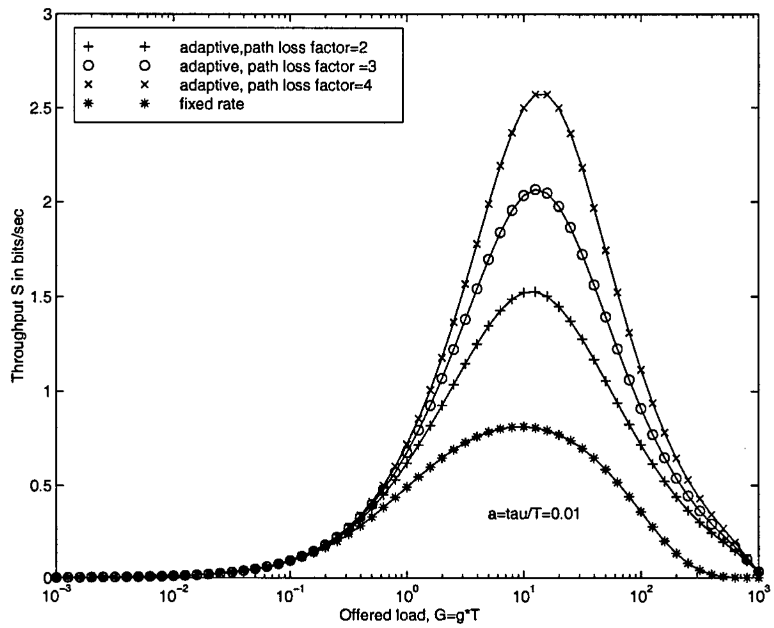

Figure 4.13: Throughput analysis, CSMA system, various path loss model

4.4 Conclusion

In this chapter, we analyze the network throughput for an adaptive OFDM-SS system. The system adapts the processing gain to the changing channel conditions in order to achieve maximum throughput while maintaining desired BER performance. Classical throughput analysis for both the fixed and random access schemes is extended to study this adaptive system. The effect of *variable packet lengths due to variable user data rate* as well as packet error rate from AWGN has been incorporated into our analysis. System throughput at the data link layer has been greatly improved compared to conventional fixed rate system.

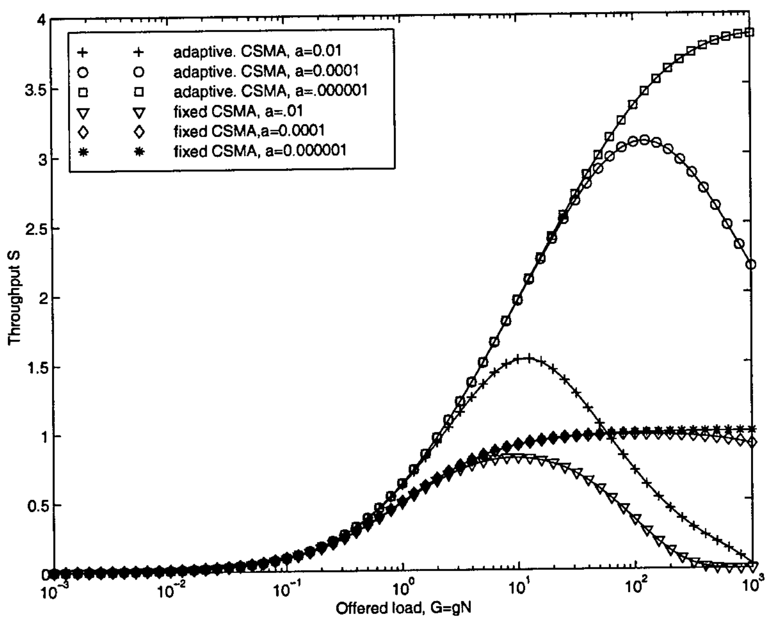

Figure 4.14: Throughput-Load of CSMA under various propagation time, linear user profile

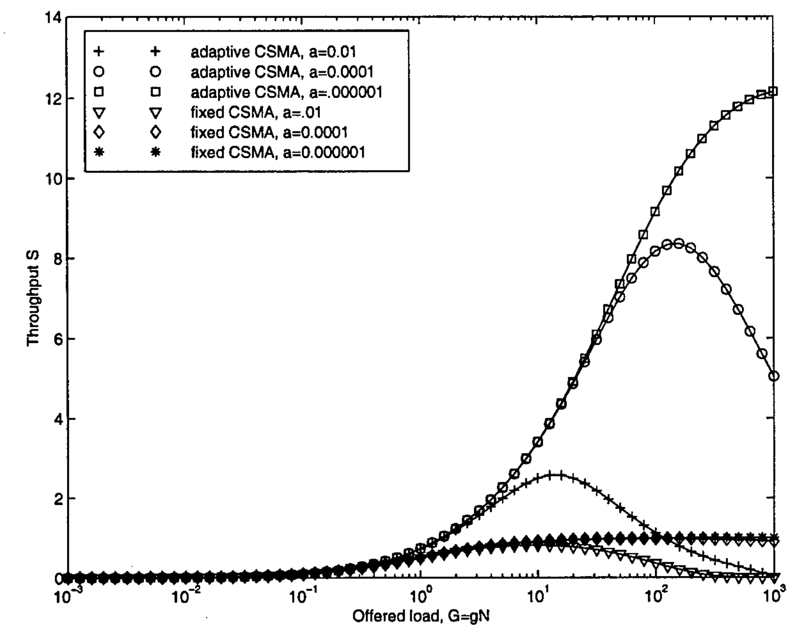

Figure 4.15: Throughput-Load of CSMA under various propagation time, flat user profile

Chapter 5

Conclusion

This report makes several important contributions to the field of tactical packet radio network designs. The major contribution is the development of the *rate adaptive spread spectrum OFDM system* which achieves the ultimate goal of maintaining a desired performance across a broad range of channel conditions by the proper control of the system processing gain. Our adaptive signaling is compared with other conventional adaptive modulation schemes and it is shown to be a simple and universal scheme across large variation of received signal quality. In particular, it is demonstrated to be especially well suited for power limited link such as satellite communications and LPI/LPD driven tactical applications. The rate adaptation strategy, associated with an optimum combination of FEC coding and spreading, is shown to be practical to implement and it has many potential applications for both commercial and military communications. In addition, the RA-OFDM scheme is further justified by analyzing the network throughput for a packet radio network. We introduced a method to analyze network throughput using *variable packet lengths due to variable user data rate.*

Bibliography

[1] US ARMY. *Army Digitization Master Plan '96.* Pentagon, 1996.

[2] E. K. Wesel. *Wireless Multimedia Communications, Networking Video, Voice, and Data.* Addison Wesley, 1997.

[3] Proakis J. G. *Digital Communications.* McGraw-Hill, 1995.

[4] J.D. Laster and J.H. Reed. Interference rejection in digital wireless communications. *IEEE Signal Processing Magazine*, 32(5), May 1997.

[5] M. K. Simon, J. K. Omura, R. A. Scholtz, and B. K. Levitt. *Spread Spectrum Communications Handbook.* McGraw-Hill, 1994.

[6] R. Price and P.E. Green. A communication technique for multipath channels. *Proceedings of IRE*, 46:555–570, March 1958.

[7] L. B. Milstein. Interference rejection techniques in spread spectrum communications. *Proceedings of the IEEE*, 76:657–671, June 1988.

[8] F. Amoroso. Techniques to improve anti-jam performance of spread spectrum systems. In *1996 IEEE 4th International Symposium on Spread Spectrum Techniques and Applications Proceedings*, pages 636–646, September 1996.

[9] B. Hirosaki. An analysis of automatic equalizers for orthogonally multiplexed QAM systems. *IEEE Transactions on Communications*, (1), January 1980.

[10] O. van de Wiel and L. Vandendorpe. Adaptive equalization structures for multitone CDMA systems. In *5th IEEE International Symposium on Personal, Indoor and Mobile Radio Communications (PIMRC'94)*, pages 253–257, September 1994.

[11] Hongnian Xing and P. Jarske. Frequency domain equalization for the multicarrier spread spectrum system in multipath fading channel. In *1996 International Conference on Communication Technology Proceedings*, pages 603–606, May 1996.

[12] M. Itami, H. Takano, H. Ohta, and K. Itoh. A method of equalization of OFDM signal with inter-symbol and inter-channel interferences. In *Proceedings of ICCS '94*, pages 109–113, November 1994.

[13] Qin L. and Bellanger M.G. Adaptive sub-channel equalization in multicarrier transmission. In *Proceedings of IEEE ICASSP'97*, pages 2321–2324, April 1997.

[14] S. B. Weinstein and P. M. Ebert. Data transmission by frequency-division multiplexing using the discrete fourier transform. *IEEE Transactions on Communication Technology*, COM-19(5), October 1971.

[15] European Telecommunication Standard. Radio broadcast systems: digital audio broadcasting (DAB) to mobile, portable and fixed receivers. *ETSI final draft*, November 1994.

[16] W. Y. Chen and D. L. Waring. Applications of ADSL to support video dial tone in the copper loop. *IEEE Communications Magazine*, 32(5), May 1994.

[17] H. Sari, G. Karam, and I. Jeanclaude. Transmission techniques for digital terrestrial TV broadcasting. *IEEE Communications Magazine*, 33(2), Feburary 1995.

[18] G. K. Kaleh. Frequency-diversity spread-spectrum communication system to counter bandlimited Gaussian interference. *IEEE Transactions on Communications*, 44(7):886–893, July 1996.

[19] G. J. Saulnier, V. A. A. Whyte, and M. J. Medley. OFDM spread spectrum communications using lapped transforms and interference excision. In *IEEE International Conference on Communications Conference Record*, pages 944–948, 1997.

[20] G. J. Saulnier, M. Mettke, and M. J. Medley. Performance of an OFDM spread spectrum communication system using lapped transforms. In *Conference Record of the IEEE Military Communications Conference*, 1997.

[21] G. J. Saulnier, Z. Ye, and M. J. Medley. Performance of a spread spectrum OFDM system in a dispersive fading channel with interference. In *Conference Record of the IEEE Military Communications Conference*, 1998.

[22] B. Fettweis, A. S. Bahai, and K. Anvari. On multi-carrier code division multiple access (MC-CDMA) modem design. In *Proceedings of the IEEE Vehicular Technology Conference*, pages 1670–1674, 1994.

[23] A. Oppenheim and R. Schafer. *Dicrete-Time Signal Processing.* Prentice-Hall, Inc, 1989.

[24] Rinne J. and Renfors M. An improved equalizing scheme for orthogonal frequency division multiplexing systems for time-variant channels. In *Proceedings of Globecom '95*, pages 879–883, 1995.

[25] Rinne J. An equalization method using preliminary decisions for orthogonal frequency division multiplexing systems in channels with frequency selective fading. In *Proceedings of the IEEE 46th Vehicular Technology Conference*, pages 1579–1583, 1996.

[26] J.K. Caver. Variable rate transmission for Rayleigh fading channels. *IEEE Transactions on Communications*, February 1972.

[27] Webb W.T. and Hanzo L. *Modern Quadrature Amplitude Modulation.* Pentech Press, 1994.

[28] Torrance J.M. and Hanzo L. Adaptive modulation in a slow Rayleigh fading channel. In *Proceedings of the IEEE PIMRC'96*, pages 497–501, 1996.

[29] Chua S.G. and Goldsmith A. Variable-rate variable-power M-QAM for fading channel. In *Proceedings of the IEEE 46th Vehicular Technology Conference*, pages 815–819, 1996.

[30] Alouini M. and Goldsmith A. Capacity of Nakagami multipath fading channel. In *Proceedings of the IEEE Vehicular Technology Conference*, pages 358–362, 1997.

[31] Ue T., Sampei S., and Morinaga N. Symbol rate and modulation level controlled adaptive modulation/TDMA/TDD for personal communica-

tions systems. In *Proceedings of the IEEE Vehicular Technology Conference*, pages 306–310, 1995.

[32] Kalet I. The multitone channel. *IEEE Transactions on Communications,* (2), Feburary 1989.

[33] Czylwik A. Adaptive OFDM for wideband radio channels. In *Conference Record of the IEEE Globecom '96*, pages 713–718, 1996.

[34] Willink T.J. and Wittke P.H. Optimization and performance evaluation of multicarrier transmission. *IEEE Transactions on Information Theory,* (2), March 1997.

[35] Chow P. and Cioffi J. Bandwidth optimization for high speed data transmission over channels with severe intersymbol interference. In *Proceedings of the IEEE Globecom '92*, pages 59–63, 1992.

[36] G. J. Saulnier, Z. Ye, and M. J. Medley. Anti-jam, anti-multipath adaptive OFDM spread spectrum system. In *Conference Record of Thirty Second Annual Asilomar Conferrence on Signals, Systems and Computers*, 1998.

[37] F. Gfeller and U. Bapst. Wirelesss in-house data communication via diffuse infrated radiation. *IEEE Proceedings*, 67, November 1979.

[38] P. Ferert. Application of spread spectrum radio to wireless terminal communications. In *Proceeding of NTC, Houston*, 1980.

[39] M. Marcus. Recent U.S. regulatory decisions on civil uses of spread spectrum. In *Proceeding of NTC, HoustonIEEE Globecom*, 1985.

[40] M. Marcus. Regulatory policy considerations for radio local area networks. *IEEE Communications Magazine*, 25(7), July 1987.

[41] T.A. Freeburg. Enabling technologies for wirelesss in-building network communications-four technical challenges, four solutions. *IEEE Communications Magazine*, 29(4), April 1991.

[42] B. Tuch. An ISM band spread spectrum local area network: Wavelan. In *IEEE Workshop on Wireless Local Area Networks*, 1991.

[43] J. Barry, J. Kahn, E. Lee, and D. Messerschmitt. High-speed nondirective optical communication for wireless networks. *IEEE Network Magazine*, 29, November 1991.

[44] V. Hayes. Wireless LANs-standard activities in IEEE. In *IEEE Workshop on Wireless Local Area Networks*, 1991.

[45] V. Hayes. Standardization efforts for wirelesss LANs. *IEEE Network Magazine*, 29, November 1991.

[46] Rinne J. and Renfors M. Equalization of orthogonal frequency division multiplexing signals. In *Proceedings of Globecom '94*, pages 415–419, 1994.

[47] Li. Y., Cimini L.J., and Sollenberger N.R. Robust channel estimation for OFDM systems with rapid dispersive fading channels. *IEEE Transactions on Communications*, (7), July 1998.

[48] G. J. Saulnier, Z. Ye, and M. J. Medley. Joint interference suppression and multipath mitigation in direct sequence and OFDM spread spectrum systems. In *Conference Record of Seventh Communication Theory Mini-Conference*, 1998.

[49] G. Santella. OFDM with guard interval and sub-channel equalization in a 2- resolution transmission scheme for digital television broadcasting. In *Conference Record,ICC/SUPERCOMM'94*, pages 374–380, May 1994.

[50] C.E. Shannon. A mathematical theory of communication. *Bell Syst. Tech. J.*, 27, July 1948.

[51] C.E. Shannon. A mathematical theory of communication. *Bell Syst. Tech. J.*, 27, October 1948.

[52] C.E. Shannon. Communication in the presense of noise. *Proc. IRE*, 37, January 1949.

[53] Gilbert E.N. Capacity of a burst-noise channel. *Bell Syst. Tech. J.*, 39, September 1960.

[54] Elliott E.O. Estimates of error rates for codes on burst-noise channels. *Bell Syst. Tech. J.*, 42, September 1963.

[55] Wang H.S. and Moayeri N. Finite-state Markov channel–A useful model for radio communication channels. *IEEE Transactions on Vehicular Technology*, 44(1), February 1995.

[56] Abramson N. The ALOHA system–another alternative for computer communications. In *AFIPS Conference Proceeding*, pages 281–285, 1970.

[57] Abramson N. and Kuo F. *The ALOHA system.* Prentice-Hall, 1973.

[58] Onozato Y. Kobayaski H. and Huynh D. An approximate method for design and analysis of an ALOHA system. *IEEE Transactions on Communications*, (1), January 1977.

[59] Leung V.C.M. and Donaldson R.W. Effects of channel errors on the delay throughput performance and capacity of ALOHA multiple access systems. *IEEE Transactions on Communications*, (5), May 1986.

[60] Kleinrock L. and Tobagi F.A. Carrier sense multiple access for packet switched radio channels. In *Proceedings of the IEEE ICC '74*, pages 21B–1–21B–7, 1974.

[61] Kleinrock L. and Tobagi F.A. Packet switching in radio channels, Part I:Carrier sense multiple access modes and their throughput-delay characteristics. *IEEE Transactions on Communications*, (12), December 1975.

[62] Abramson N. The throughput of packet broadcasting channels. *IEEE Transactions on Communications*, (1), January 1977.

[63] Ferguson M.J. A stufy of unslotted ALOHA with variable packet lengths. In *Proceedings of DATACOMM*, pages 5.20–5.25, 1975.

[64] Bellini S. and Borgonovo P. On the throughput of an ALOHA channel with variable packet lengths. *IEEE Transactions on Communications*, (11), November 1977.

[65] Heyman D.P. The effects of random message sizes on the performance of CSMA/CD protocol. *IEEE Transactions on Communications*, (6), June 1986.

[66] Roberts J.A. and Healy T.J. Packet radio performance over slow fading channels. *IEEE Transactions on Communications*, (2), February 1980.

[67] Rappaport T. *Wireless Communications*. Prentice Hall, 1996.

[68] M.L. Molle, K. Sohraby, and A.N. Venetsanopoulos. Space-time models of asynchronous CSMA protocols for local area networks. *IEEE Journal on Selected Areas in Communications*, (6), July 1987.

[69] D. Bertsekas and R. Gallager. *Data Networks.* Prentice Hall, 1992.

[70] Lee W.C.Y. *Mobile Communications Engineering.* McGraw Hill, 1985.

☆U.S. GOVERNMENT PRINTING OFFICE: 1999-510-079-81210